

Supporting Information

Translocation of Intracellular Proteins via Peptide-Directed Ligation

Christiane Stiller^{1,2}, Dennis M. Krüger^{1,2}, Nicolas Brauckhoff¹, Marcel Schmidt¹, Petra Janning³, Hazem Salamon¹, Tom N. Grossmann^{1-4,*}

¹ Chemical Genomics Centre of the Max Planck Society, Otto-Hahn-Str. 15, 44227 Dortmund, Germany.

² Technical University Dortmund, Department of Chemistry and Chemical Biology, Otto-Hahn-Str. 6, 44227 Dortmund, Germany.

³ Max Planck Institute of Molecular Physiology, Otto-Hahn-Str. 11, Dortmund, Germany.

⁴ VU University Amsterdam, Department of Chemistry & Pharmaceutical Sciences, De Boelelaan 1083, 1081 HV, Amsterdam (The Netherlands).

* Correspondence to Dr. Tom N. Grossmann, Professor of Organic Chemistry, VU University Amsterdam, Department of Chemistry & Pharmaceutical Sciences, De Boelelaan 1108, 1081 HZ, Amsterdam (The Netherlands), Email: t.n.grossmann@vu.nl

1 SI FIGURES

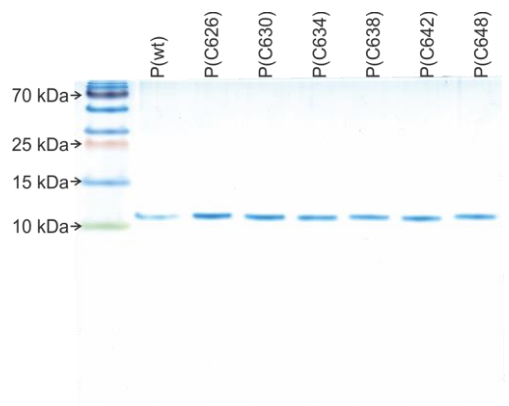


Figure S1: Analytical SDS-PAGE of all seven protein P variants. All proteins **P** show very good purity. 10 μL of each protein ($c = 0.5 \mu\text{g} \cdot \mu\text{L}^{-1}$) were mixed with 2 μL of 5x SDS loading buffer (62.5 mM Tris pH 6.8, 2% SDS, 5% β -Me, 10% Glycerol, 1% Coomassie Brilliant Blue) and heated to 95°C for 5 min. Afterwards they were loaded onto a 17% SDS-PAGE gel (Tris-Tricin according to Schägger and Jagow¹), which was run at 100 V for 1.5 h.

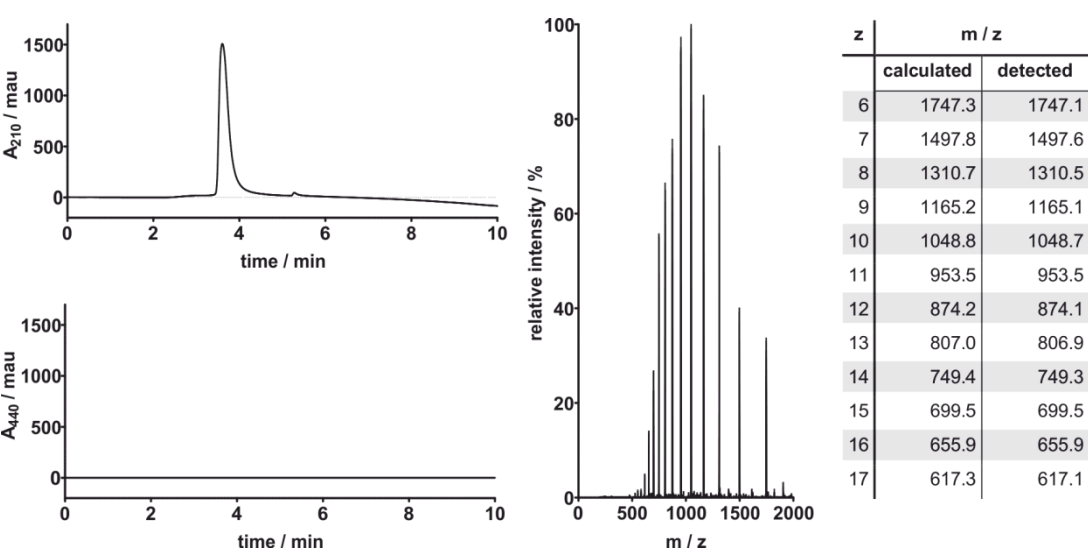


Figure S2: Analytical HPLC-MS measurement with UV/Vis-detection of **P(wt)**. Left: Chromatograms of the HPLC (30-95% solvent B in 10 min. Solvent A: 0.1% TFA in H_2O , solvent B: 0.1% TFA in ACN) at 210 nm (upper panel, absorption of peptide bonds) and 440 nm (lower panel, absorption of **f** in acidic milieu). Middle: mass spectrum of the highest peak of the 210 nm chromatogram. Right: Calculated and detected m/z-values. Deconvolution software from Agilent Technologies (Santa Clara, California, USA) found a protein mass of 10476.87, which is in good agreement with the calculated mass 10477.90 using ProtParam.²

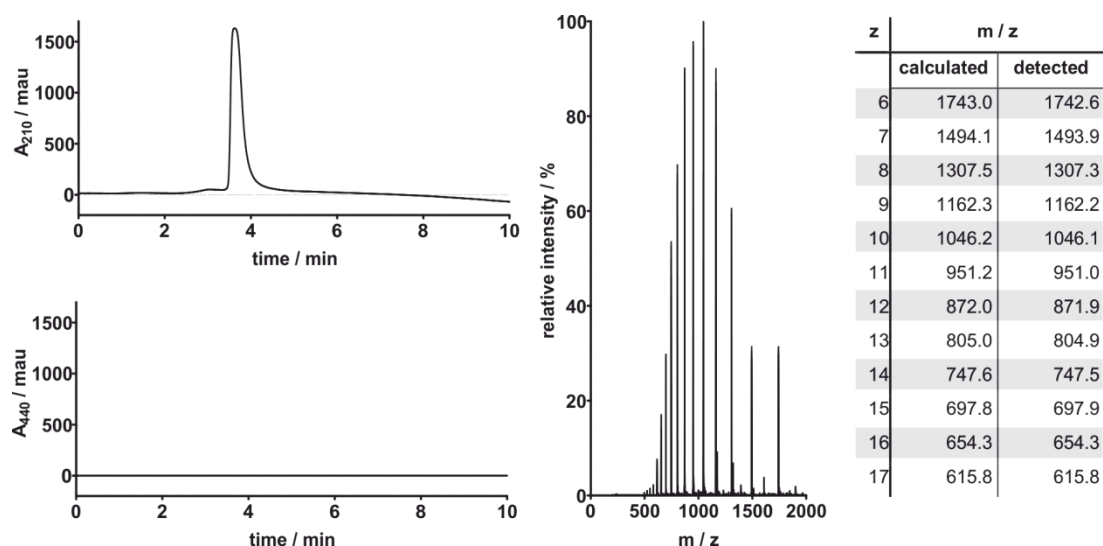


Figure S3: Analytical HPLC-MS measurement with UV/Vis-detection of **P(C626)**. Left: Chromatograms of the HPLC (30-95% solvent B in 10 min. Solvent A: 0.1% TFA in H₂O, solvent B: 0.1% TFA in ACN) at 210 nm (upper panel, absorption of peptide bonds) and 440 nm (lower panel, absorption of **f** in acidic milieu). Middle: mass spectrum of the highest peak of the 210 nm chromatogram. Right: Calculated and detected m/z-values. Deconvolution software from Agilent Technologies (Santa Clara, California, USA) found a protein mass of 10450.5, which is in good agreement with the calculated mass 10452.00 using ProtParam.²

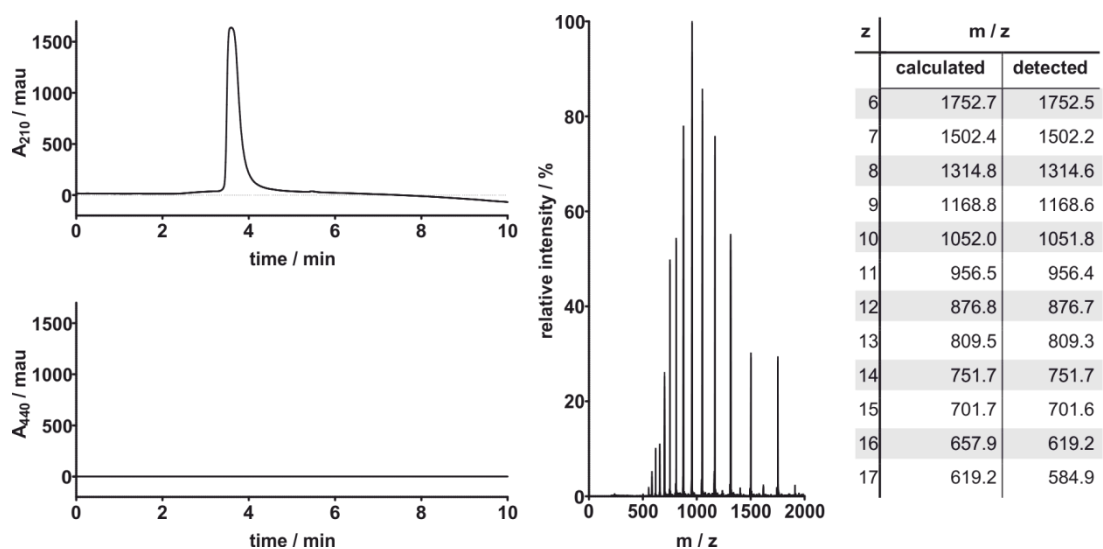


Figure S4: Analytical HPLC-MS measurement with UV/Vis-detection of **P(C630)**. Left: Chromatograms of the HPLC (30-95% solvent B in 10 min. Solvent A: 0.1% TFA in H₂O, solvent B: 0.1% TFA in ACN) at 210 nm (upper panel, absorption of peptide bonds) and 440 nm (lower panel, absorption of **f** in acidic milieu). Middle: mass spectrum of the highest peak of the 210 nm chromatogram. Right: Calculated and detected m/z-values. Deconvolution software from Agilent Technologies (Santa Clara, California, USA) found a protein mass of 10508.71, which is in good agreement with the calculated mass 10510.00 using ProtParam.²

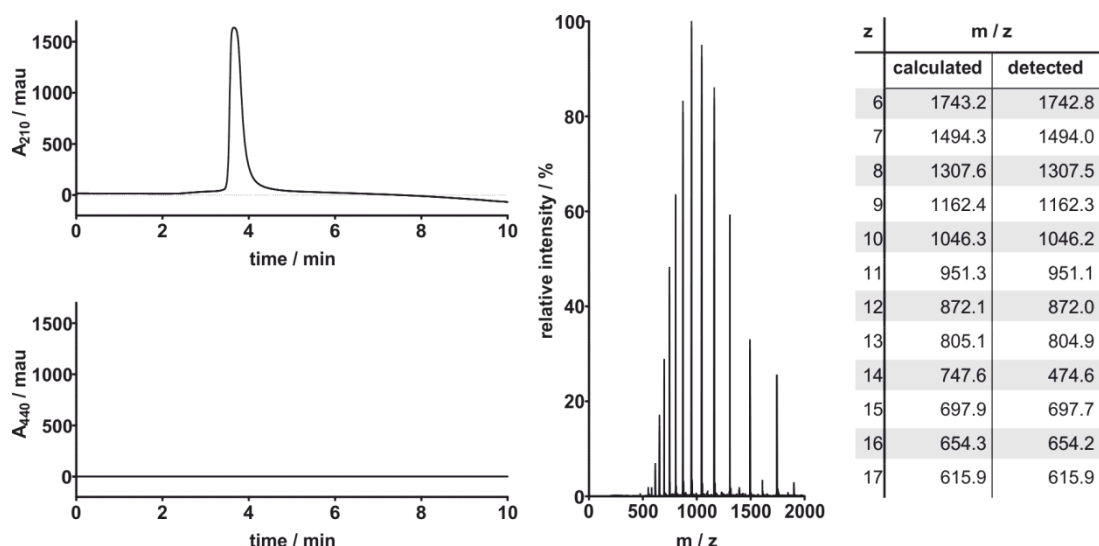


Figure S5: Analytical HPLC-MS measurement with UV/Vis-detection of **P(C634)**. Left: Chromatograms of the HPLC (30-95% solvent B in 10 min. Solvent A: 0.1% TFA in H₂O, solvent B: 0.1% TFA in ACN) at 210 nm (upper panel, absorption of peptide bonds) and 440 nm (lower panel, absorption of **f** in acidic milieu). Middle: mass spectrum of the highest peak of the 210 nm chromatogram. Right: Calculated and detected m/z-values. Deconvolution software from Agilent Technologies (Santa Clara, California, USA) found a protein mass of 10451.87, which is in good agreement with the calculated mass 10452.90 using ProtParam.²

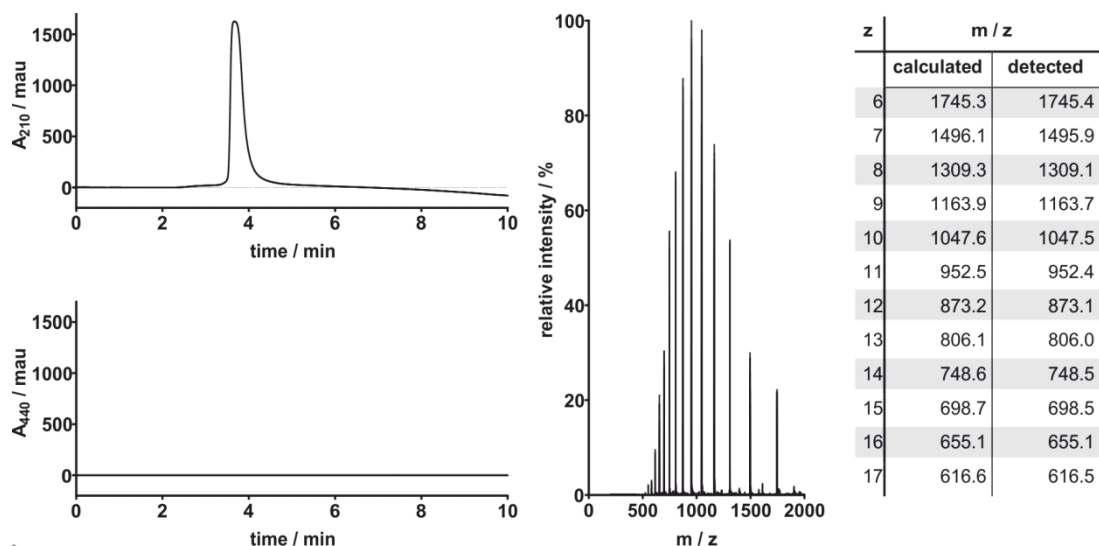


Figure S6: Analytical HPLC-MS measurement with UV/Vis-detection of **P(C638)**. Left: Chromatograms of the HPLC (30-95% solvent B in 10 min. Solvent A: 0.1% TFA in H₂O, solvent B: 0.1% TFA in ACN) at 210 nm (upper panel, absorption of peptide bonds) and 440 nm (lower panel, absorption of **f** in acidic milieu). Middle: mass spectrum of the highest peak of the 210 nm chromatogram. Right: Calculated and detected m/z-values. Deconvolution software from Agilent Technologies (Santa Clara, California, USA) found a protein mass of 10464.67, which is in good agreement with the calculated mass 10466.00 using ProtParam.²

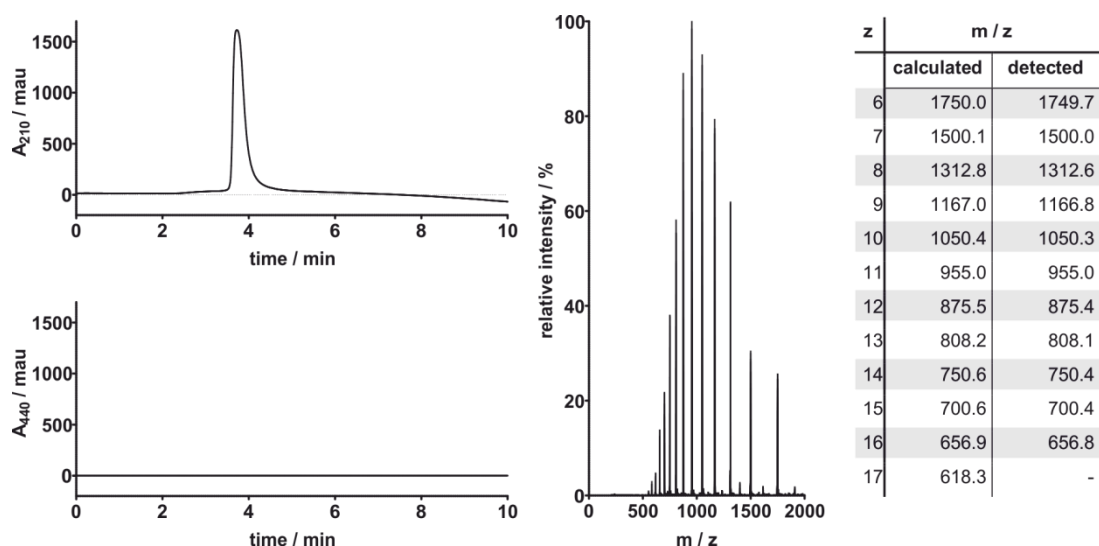


Figure S7: Analytical HPLC-MS measurement with UV/Vis-detection of **P(C642)**. Left: Chromatograms of the HPLC (30-95% solvent B in 10 min. Solvent A: 0.1% TFA in H₂O, solvent B: 0.1% TFA in ACN) at 210 nm (upper panel, absorption of peptide bonds) and 440 nm (lower panel, absorption of **f** in acidic milieu). Middle: mass spectrum of the highest peak of the 210 nm chromatogram. Right: Calculated and detected m/z-values. Deconvolution software from Agilent Technologies (Santa Clara, California, USA) found a protein mass of 10492.43, which is in good agreement with the calculated mass 10494.00 using ProtParam.²

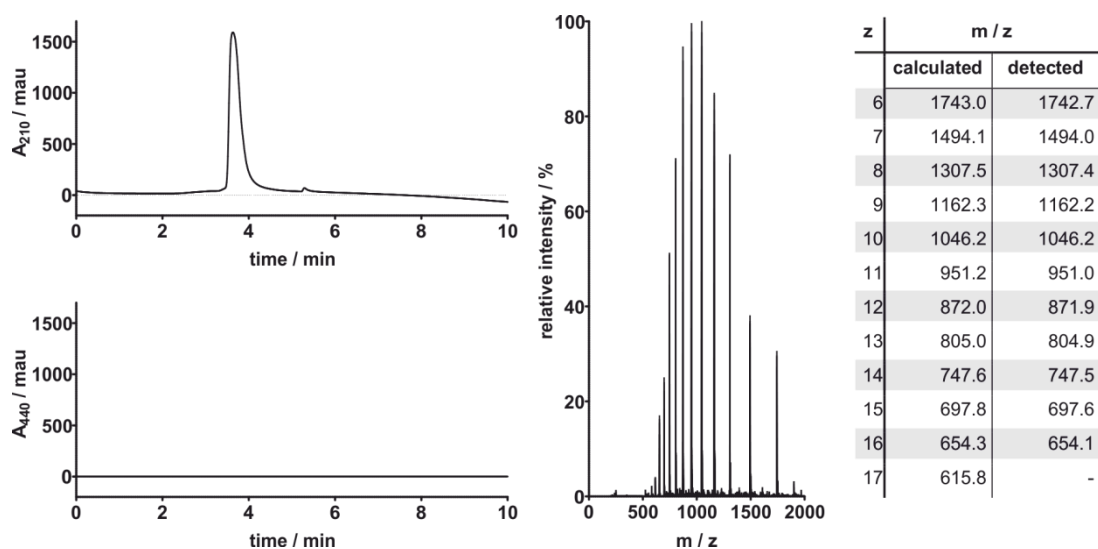


Figure S8: Analytical HPLC-MS measurement with UV/Vis-detection of **P(C648)**. Left: Chromatograms of the HPLC (30-95% solvent B in 10 min. Solvent A: 0.1% TFA in H₂O, solvent B: 0.1% TFA in ACN) at 210 nm (upper panel, absorption of peptide bonds) and 440 nm (lower panel, absorption of **f** in acidic milieu). Middle: mass spectrum of the highest peak of the 210 nm chromatogram. Right: Calculated and detected m/z-values. Deconvolution software from Agilent Technologies (Santa Clara, California, USA) found a protein mass of 10450.84, which is in good agreement with the calculated mass 10452.00 using ProtParam.²

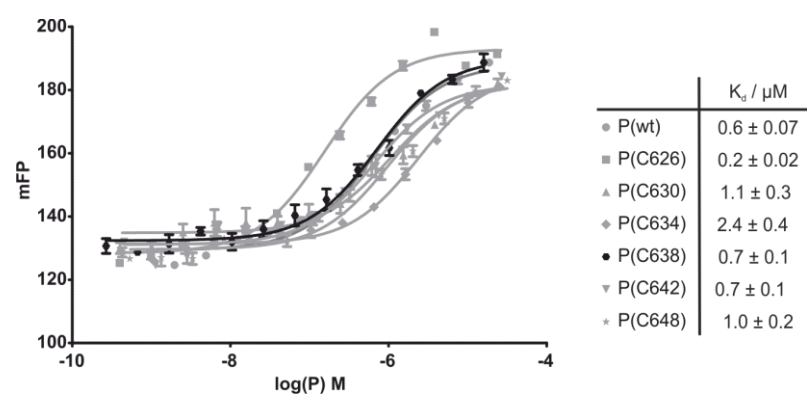


Figure S9: FP-measurement of **H-L-f** against all seven protein **P** variants. Values are obtained from triplicates. Error bars account for 1σ .

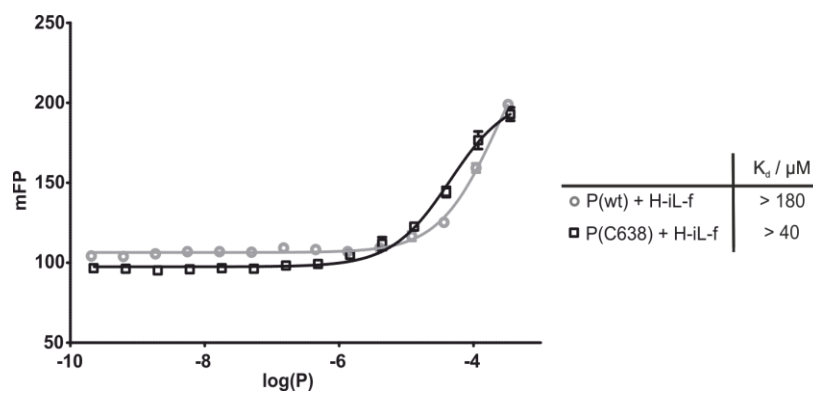


Figure S10: FP-measurements of **H-iL-f** against proteins **P(wt)** and **P(C638)**. Error bars are obtained from triplicates and account for 1σ .

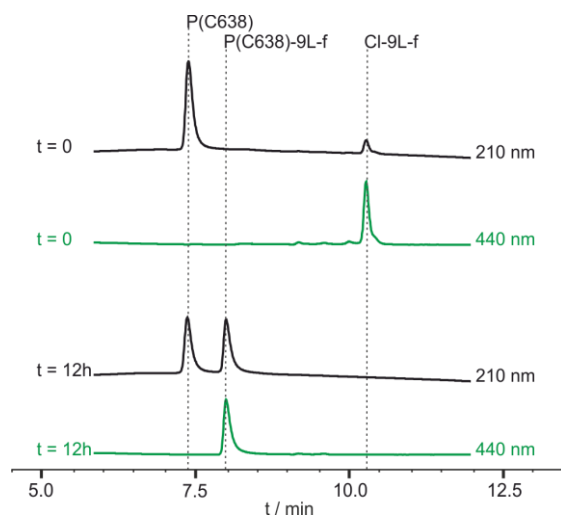


Figure S11: Exemplary HPLC chromatograms for the determination of product yields. For all reactions, UV/Vis-detection at 210 nm (absorption maximum for amide bonds) and 440 nm (absorption maximum of FITC (**f**) in the acidic milieu of the HPLC) was performed. Upper panels show the chromatograms of a quenched protein **P(C638)** with peptide ligand **CI-9L-f**. In the lower panel, the reaction of **P(C638)** (20 μ M) with **CI-9L-f** (10 μ M) is shown after 12 h. The chromatograms show a reduction of the signals corresponding to **CI-9L-f** and **P(C638)**, while a new signal for the ligation product **P(C638)-9L-f** appears.

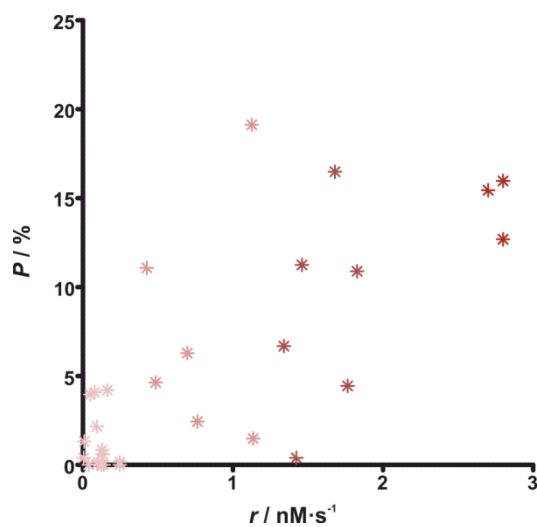


Figure S12: Scatter plot based on probability of occurrence (P) of the reacting atoms (cysteinic sulfur and α -carbon of α -chloroacetamide) within a distance of 5 Å (derived from MD, Table S9) and initial reaction rates r (Table S8) of all six proteins **P** in combination with all five ligands **L**.

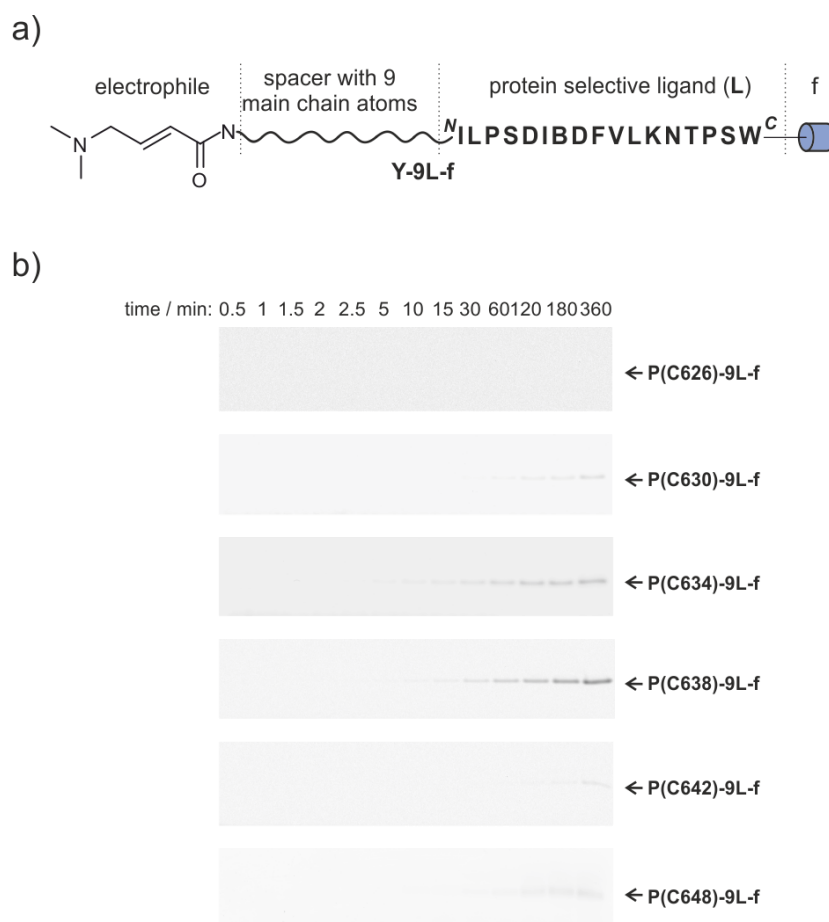


Figure S13: a) General structure of reactive probe **Y-9L-f**. b) Fluorescence readout of reactions between dimethylamino acrylamide modified ligand **Y-9L-f** with all six cysteine containing protein variants. Readout was performed on 17% SDS-PAGE gels according to Schagger and Jagow¹ and read-out of fluorescein fluorescence. Most intense product bands are observed for protein variants P(C634) and P(C638). This is in line with the results obtained from MD simulations and with the reactivity of α -chloroacetamide-modified peptide bearing the same linker (**Cl-9L-f**).

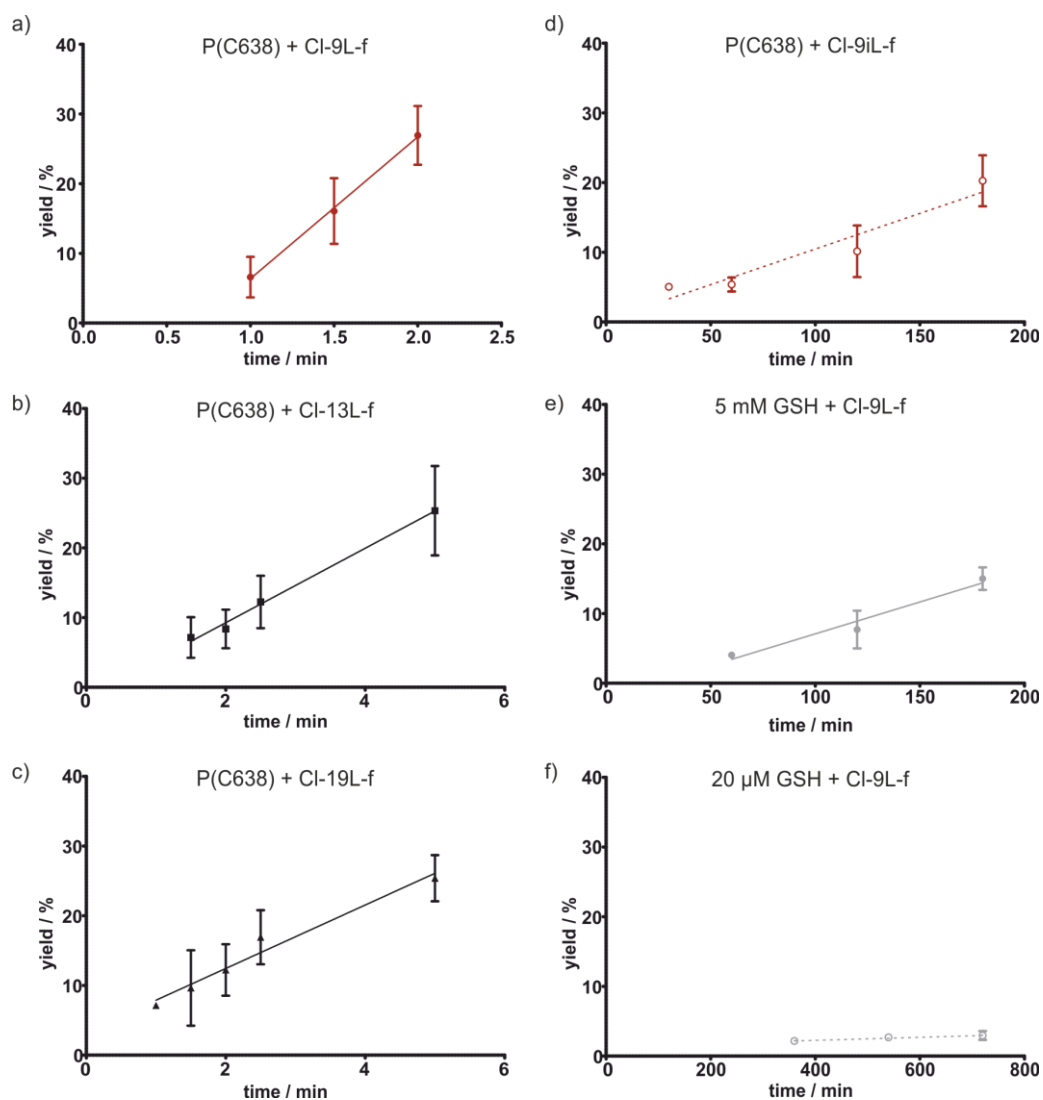


Figure S14: Linear fit of data obtained from three independent measurements. Initial rates (r) are based on slope of these fits via equation 1. a) **P(C638)+Cl-9L-f:** $v = 34 \pm 2 \text{ nM}\cdot\text{s}^{-1}$, b) **P(C638)+Cl-13L-f:** $v = 8.9 \pm 0.6 \text{ nM}\cdot\text{s}^{-1}$, c) **P(C638)+Cl-19L-f:** $v = 7.6 \pm 0.8 \text{ nM}\cdot\text{s}^{-1}$, d) **P(C638)+Cl-9iL-f:** $v = 0.17 \pm 0.04 \text{ nM}\cdot\text{s}^{-1}$, e) **5 mM GSH + Cl-9L-f:** $v = 0.15 \pm 0.03 \text{ nM}\cdot\text{s}^{-1}$, f) **20 μ M GSH + Cl-9L-f:** $v = 0.0036 \pm 0.0007 \text{ nM}\cdot\text{s}^{-1}$.

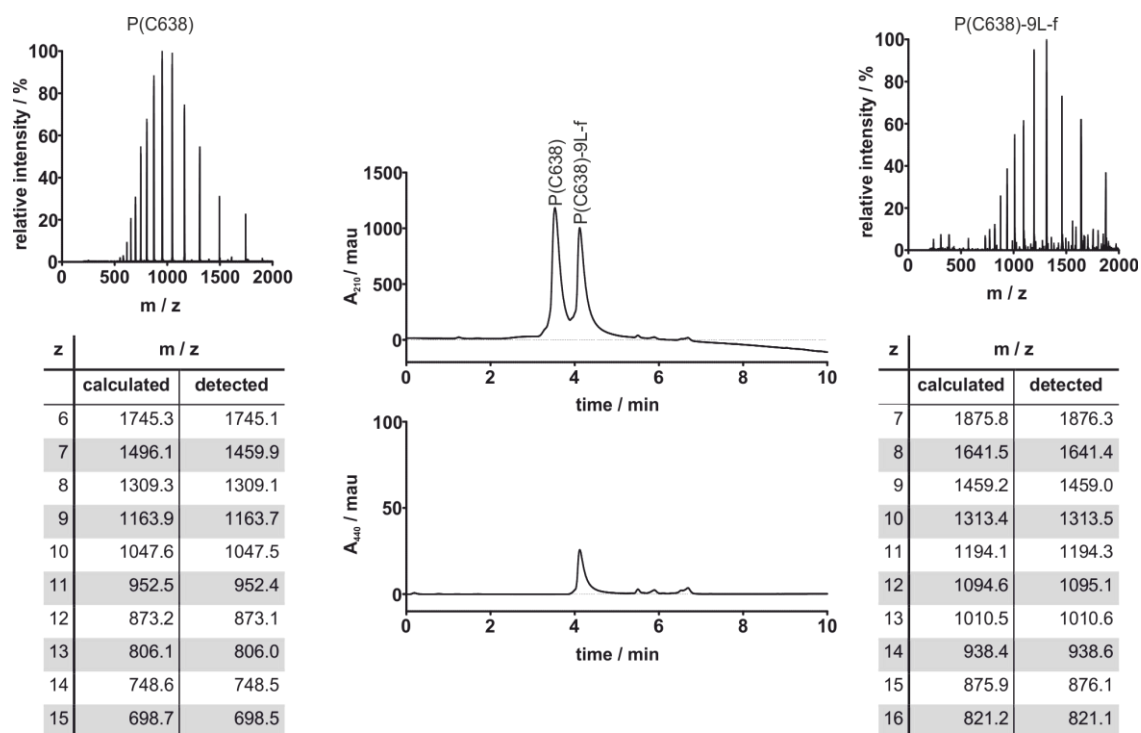


Figure S15: Analytical HPLC-MS measurement with UV/Vis-detection of P(C638)-9L-f. Chromatograms of the HPLC (10-90% solvent B in 20 min, solvent A: 0.1% TFA in H₂O, solvent B: 0.1% TFA in ACN) at 210 nm (upper panel) and 440 nm (lower panel) as well as mass spectra obtained from the two protein peaks, representing unmodified **P(C638)** (left) and conjugate **P(C638)-9L-f** (right).

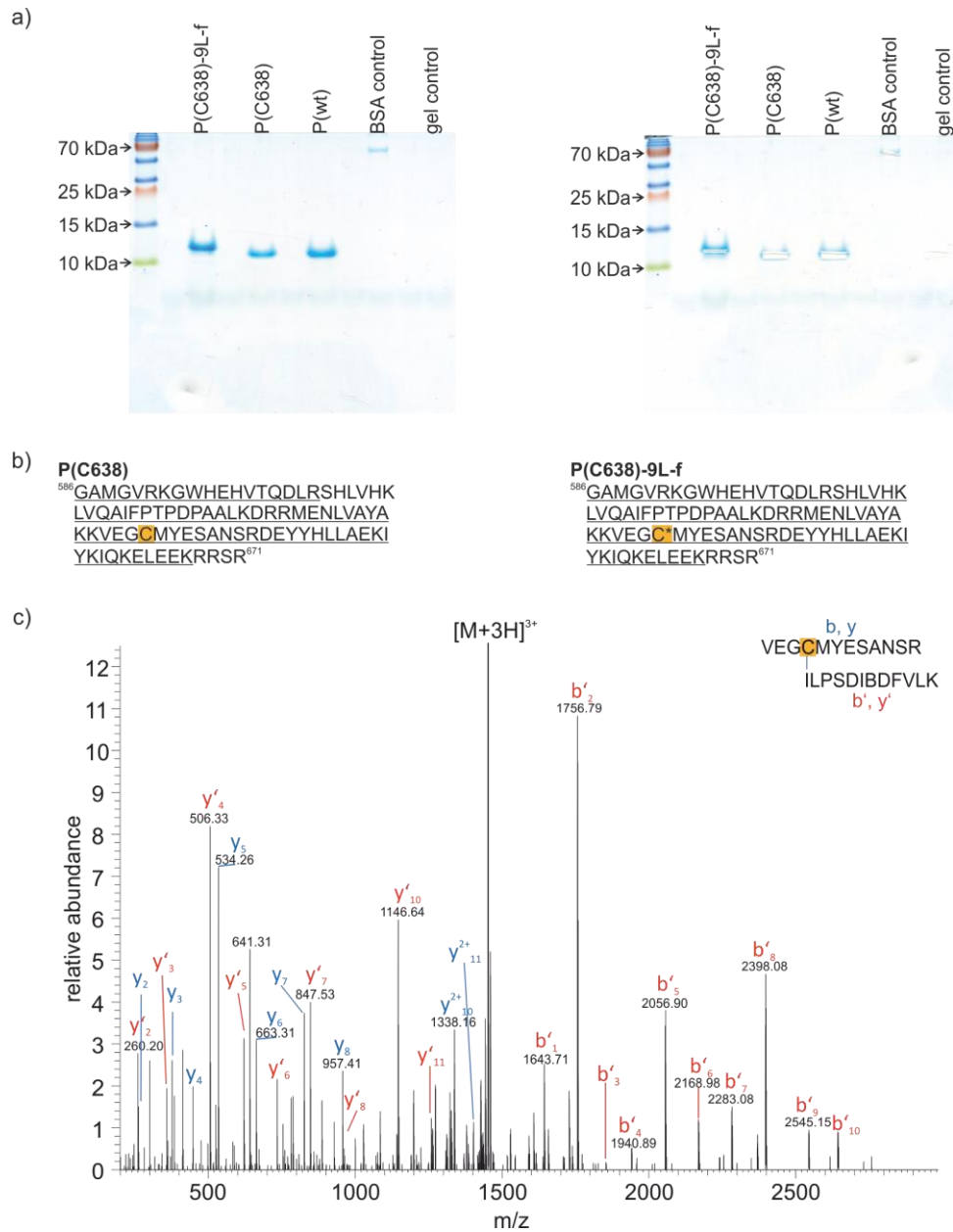


Figure S16: a) Gel for in gel digest and HPLC-MS/MS-analysis of **P(C638)** in conjugation with **CI-9L-f**. Gel is shown before (left) and after (right) cutting of sample bands for further treatment. b) Sequence coverage of proteins **P** and **P(C638)**. Modification of **P(C638)** does not interfere with MS-MS measurement. c) MS-MS analysis of a fragment of protein **P(C638)** labeled with trypsin cut peptide **CI-9L-f**.

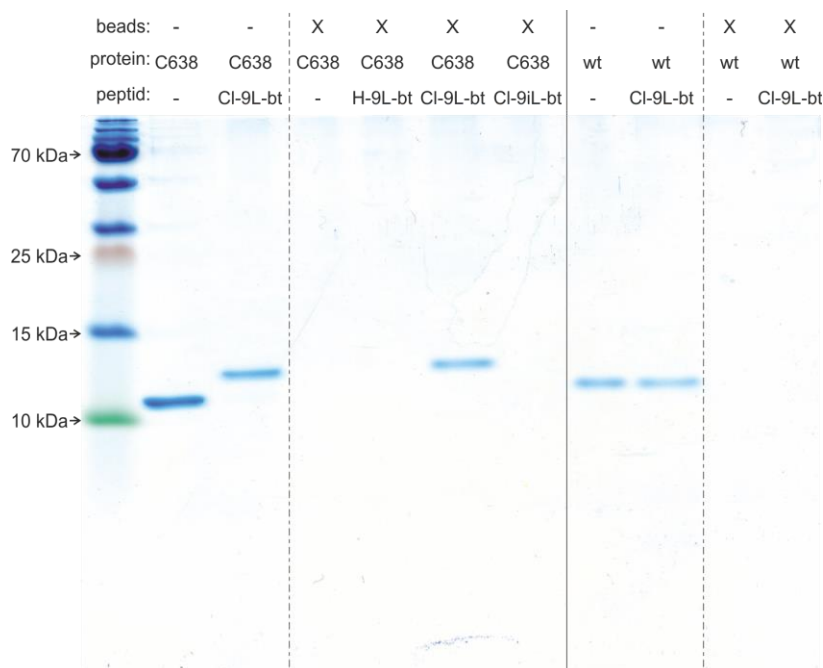


Figure S17: Coomassie stained SDS-PAGE gel (Tris-Tricin according to Schägger and Jagow¹) from the covalent pulldown of proteins **P(wt)** and **P(C638)** with ligands **H-9L-bt**, **CI-9L-bt** and **CI-9iL-bt**. In the first two lanes 5% of the input of **P(C638)** are shown. The shift to higher molecular weight upon covalent linkage to **CI-9L-bt** is clearly visible (lane 2). Lane 3 shows the control for unspecific binding of **P(C638)** to the beads. Lanes 4-6 show the actual pulldown with the three ligands. Binding and reactive probe **CI-9L-bt** (lane 5) is the only ligand able to pull **P(C638)** in detectable amounts, whereas the binding but non-reactive ligand **H-9L-bt** (lane 4) and the non-binding and reactive ligand **CI-9iL-bt** (lane 6) are unable to show efficient pulldown **P(C638)**. In lanes 7 and 8 the input samples of **P(wt)** are shown. No shift upon addition of **CI-9L-bt** occurs as this protein is unable to bind covalently to the ligand. Consequently, we do not observe pulldown in lane 10. Lane 9 shows the control for unspecific binding of **P(wt)** to the beads.

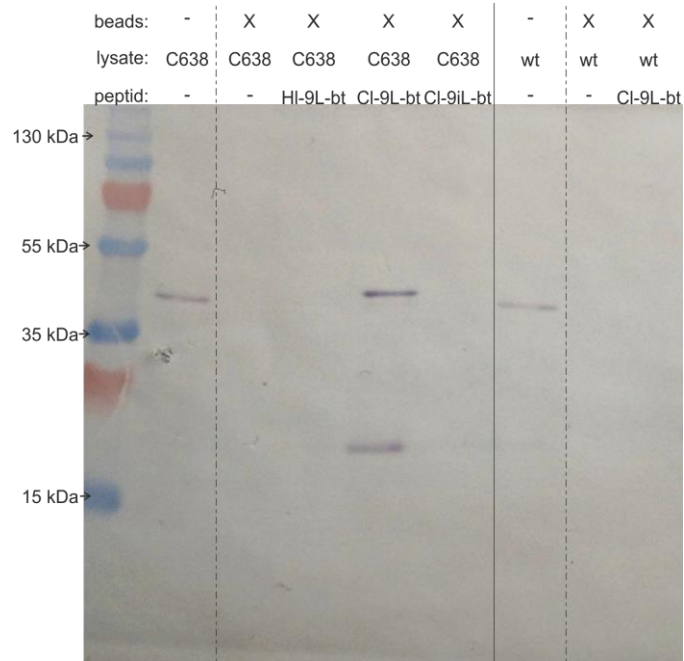


Figure S18: Nitrocellulose membrane from the covalent pulldown of proteins **P(wt)**-Cherry and **P(C638)**-Cherry from transfected Hek293 lysates with ligands **H-9L-bt**, **CI-9L-bt** and **CI-9iL-bt**. In the first lane 1% of the input from lysate containing **P(C638)** is shown. Lane 2 shows the control for unspecific binding of **P(C638)**-Cherry to the beads. Lanes 3-5 show pulldown with the three ligands. Binding and reactive ligand **CI-9L-bt** (lane 4) is the only probe able to pulldown **P(C638)** in detectable amounts, whereas the binding but non-reactive ligand **H-9L-bt** (lane 3) and the non-binding but reactive ligand **CI-9iL-bt** (lane 5) are unable to pull **P(C638)**. In lane 6, 1% of the input from **P(wt)**-Cherry containing lysate is shown. As this protein is unable to bind covalently to the probes no pull down is seen in lane 8. Lane 7 shows the control for unspecific binding of **P(wt)**-Cherry to the beads.

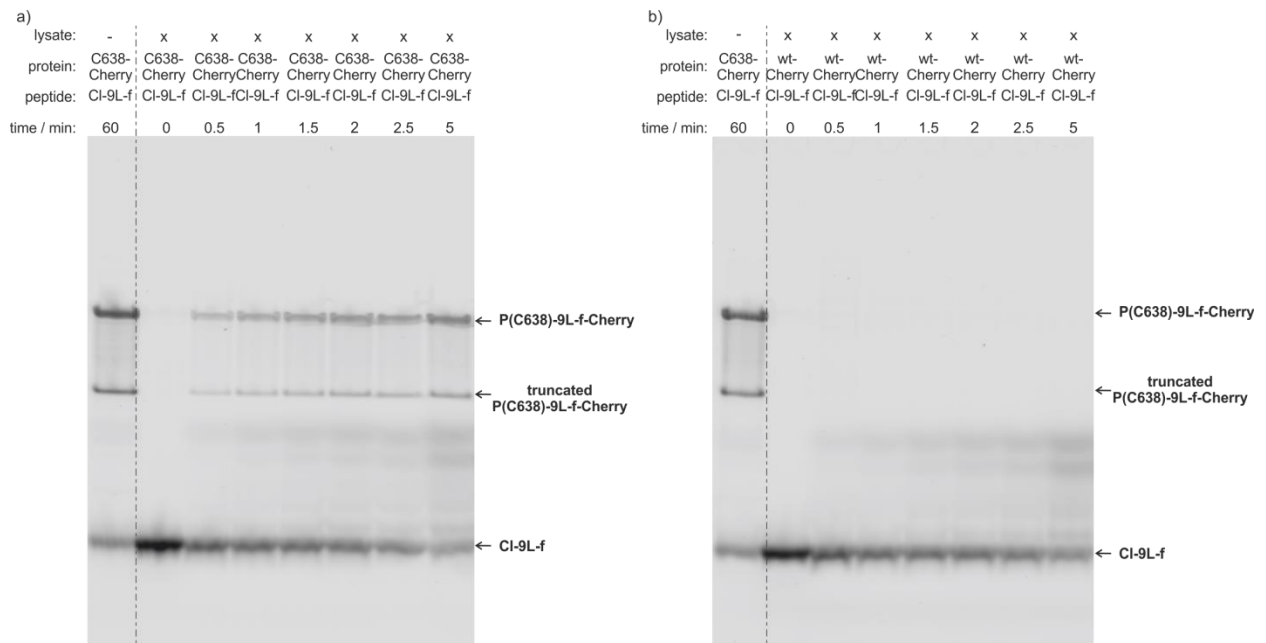


Figure S19: Labeling reactions with peptide **CI-9L-f** in *E. coli* lysates containing a) protein **P(C638)-Cherry** and b) protein **P(wt)-Cherry**. Readout was performed on 15% SDS-PAGE gels according to Schagger and Jagow¹ and read-out of fluorescein fluorescence.

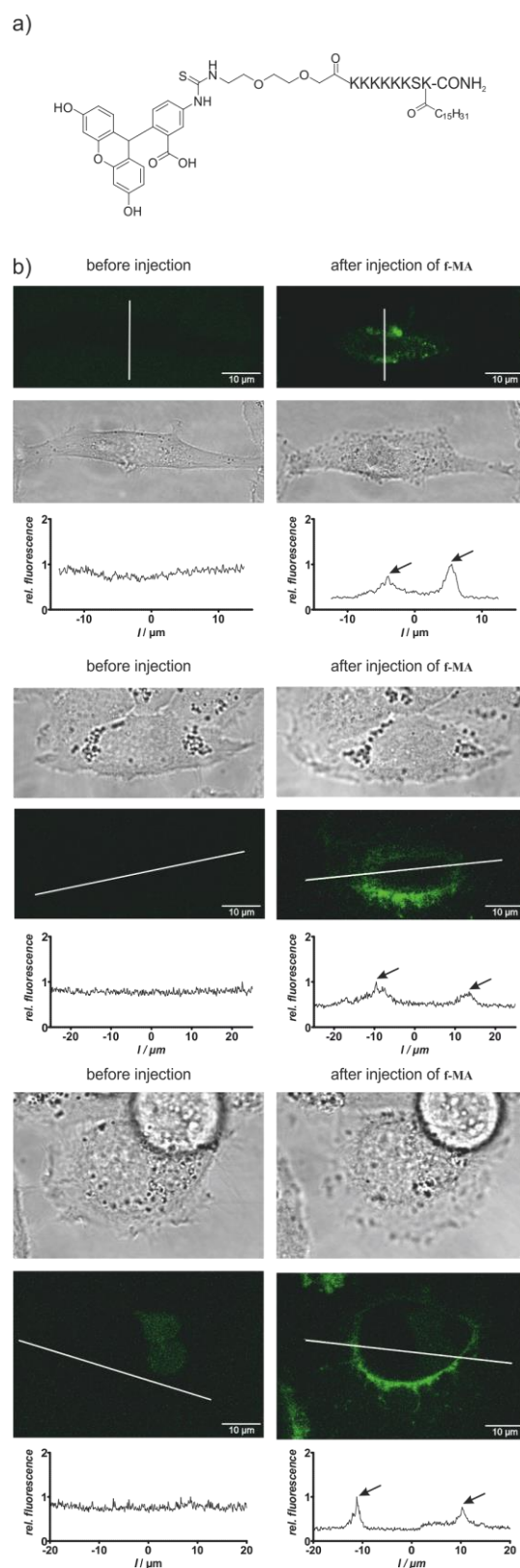


Figure S20: a) Structure of localizing peptide **f-MA**. b) confocal and transmitted-light images of three different Hek293 cells before (left panels) and after (right panels) injection of the localizing peptide **f-MA**. Top: bright field microscopy. Middle: confocal fluorescence microscopy ($\lambda_{\text{excitation}} = 488 \text{ nm}$, $\lambda_{\text{emission}} = 505 - 550 \text{ nm}$ (BP), $6.4 \mu\text{s}/\text{pixel}$). Bottom: plot of relative fluorescence intensity along white line in picture above. Peptide **f-MA** appears to localize to the endomembrane system around the nucleus.

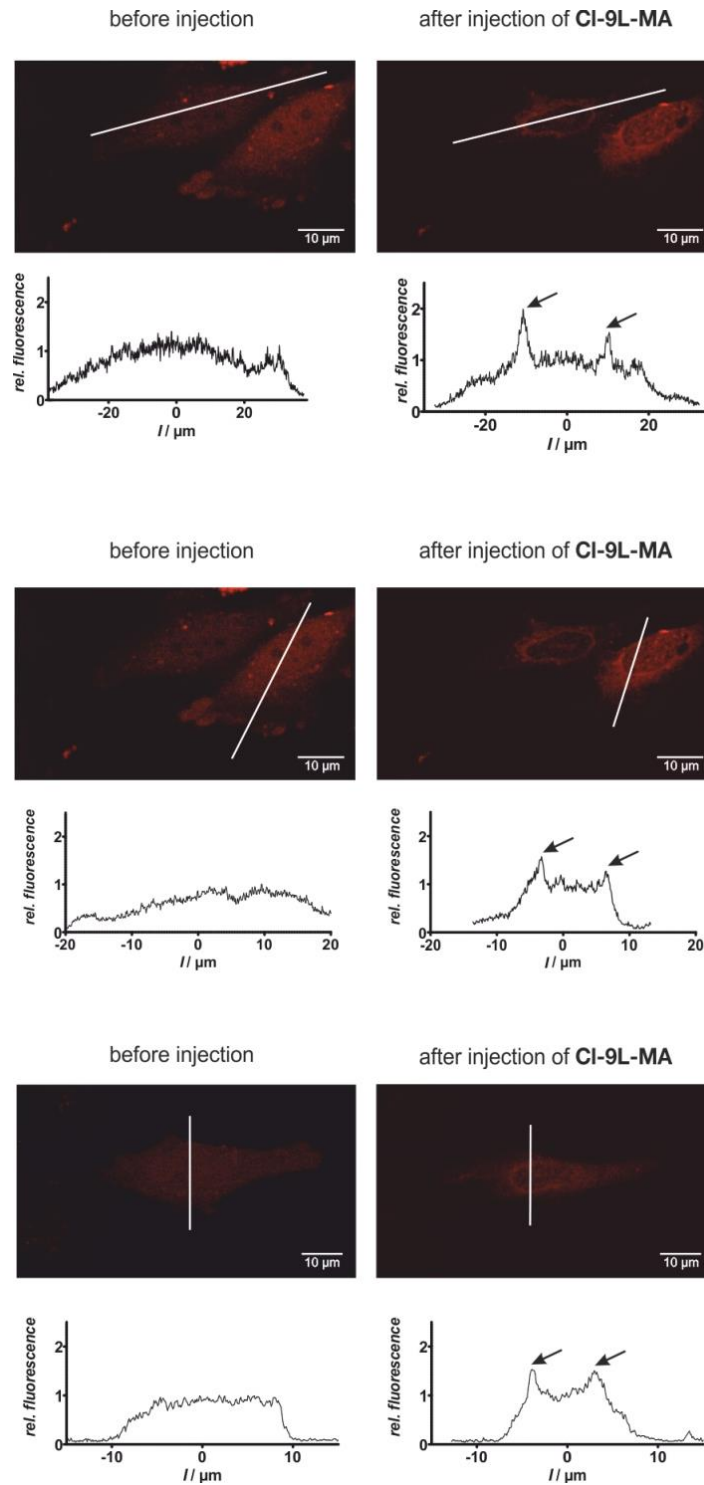


Figure S21: Live cell confocal images of three different HeLa cells transiently transfected with **P(C638)-Cherry** before (left panels) and after (right panels) injection of the affine, reactive peptide **CI-9L-MA**. Top: confocal fluorescence microscopy ($\lambda_{\text{excitation}} = 561 \text{ nm}$, $\lambda_{\text{emission}} > 575 \text{ nm}$ (LP), $6.4 \mu\text{s}/\text{pixel}$). Bottom: plot of relative Cherry fluorescence intensity along white line above (arrows indicate sites with increased localization). Peptide **CI-9L-MA** appears to localize **P(C638)-Cherry** in analogy to localization pattern observed for the labeled MA-peptide alone (Figure S20).

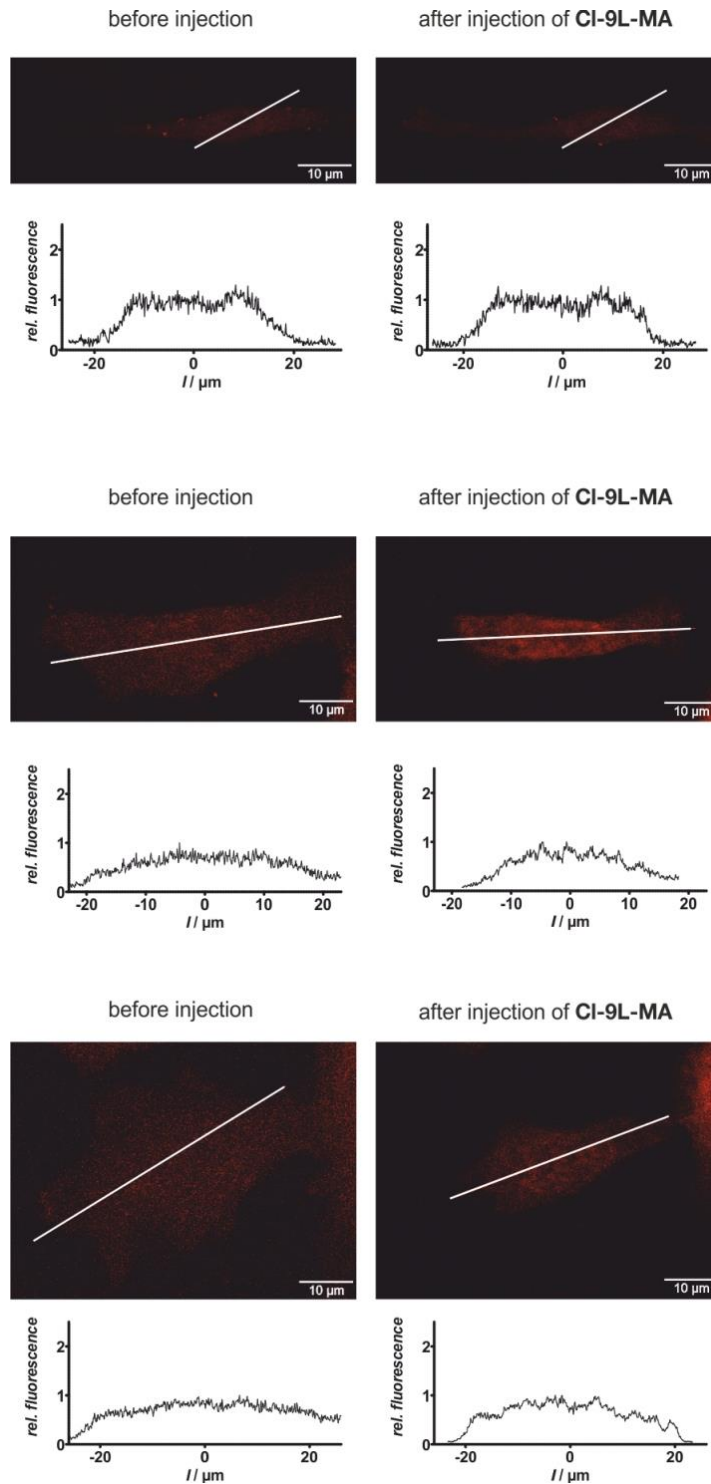


Figure S22: Live cell confocal images of three different HeLa cells transiently transfected with **P(wt)**-Cherry before (left panels) and after (right panels) injection of the affine, reactive peptide **CI-9L-MA**. Top: confocal fluorescence microscopy ($\lambda_{\text{excitation}} = 561 \text{ nm}$, $\lambda_{\text{emission}} > 575 \text{ nm}$ (LP), $6.4 \mu\text{s}/\text{pixel}$). Bottom: plot of relative Cherry fluorescence intensity along white line above. No change in **P(wt)**-Cherry localization is detectable, indicating that covalent attachment of the peptide is crucial for efficient translocation.

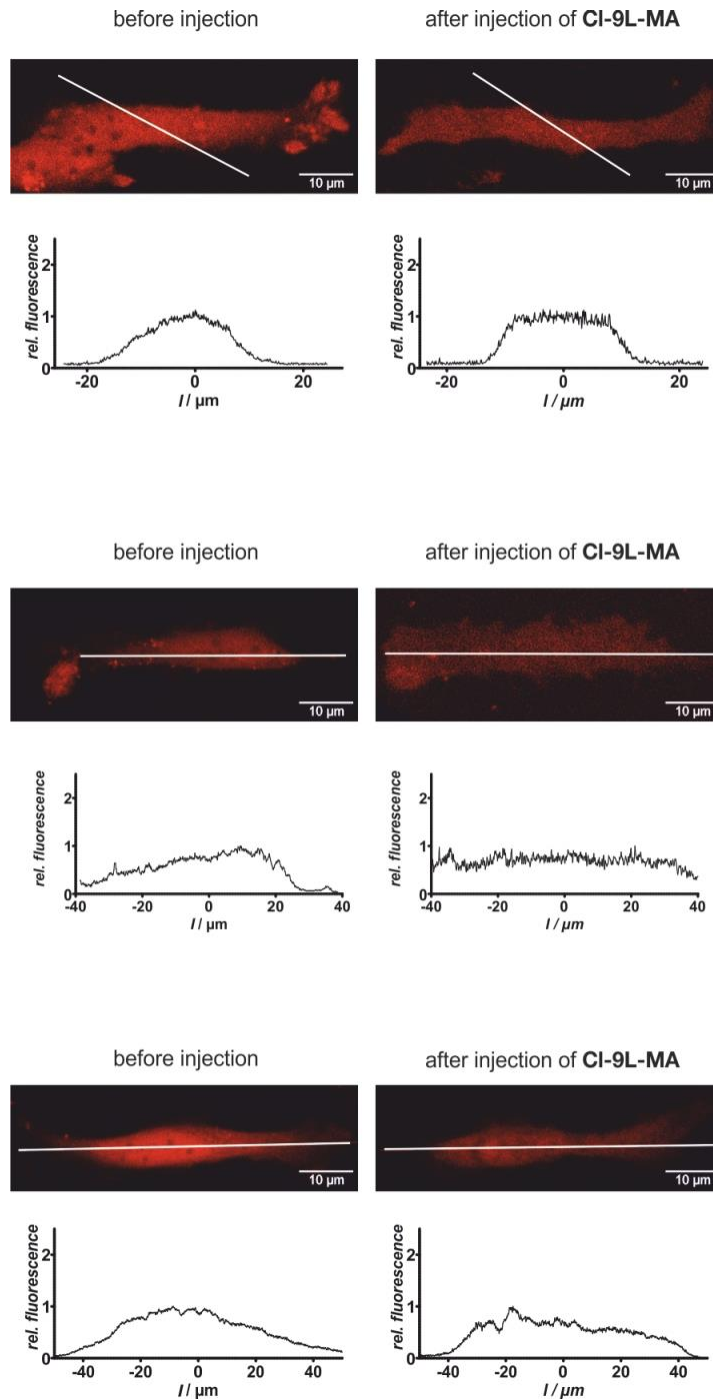


Figure S23: Live cell confocal images of three different HeLa cells transiently transfected with **P(C638)**-Cherry before (left panels) and after (right panels) injection of the less affine, reactive peptide **CI-9L-MA**. Top: confocal fluorescence microscopy ($\lambda_{\text{excitation}} = 561 \text{ nm}$, $\lambda_{\text{emission}} > 575 \text{ nm}$ (LP), $6.4 \mu\text{s}/\text{pixel}$). Bottom: plot of relative Cherry fluorescence intensity along white line above. No change in **P(C638)**-Cherry localization is detectable, indicating that the proximity-induced reaction is necessary and covalent attachment of the localizer is essential for translocation.

2 SI TABLES

Table S1: List of primers used for quick change mutagenesis (QC), restriction-ligation cloning (R-L) and sequencing of the obtained pGEX-vectors encoding for proteins **P** for expression in *E. coli* as well as Cherry vectors for expression in human cell lines. Melting temperature (T_m) and length of the primers are given. The codon introducing the desired cysteine is highlighted in yellow, restriction sides are highlighted in blue and the introduced start codon for **P-Cherry** expression is highlighted in green.

primer	sequence	T_m / °C	length / nt	used for
P(C626)_f	CTAAAGGATCGCCGATGTGCAACCTGGTAGCCTATGCTAAGAAAGTGG	73	49	QC to P(C626)
P(C626)_r	CTTAGCATAGGCTACCAGGTTGCATGCGGCGATCCTTTAGAGCT	73	46	QC to P(C626)
P(C630)_f	GCATGGAAAACCTGGTATGCTATGCTAAGAAAGTGG	66	36	QC to P(C630)
P(C630)_r	CCACTTCTTAGCATAGCAATACCAGGTTTCCATGC	66	36	QC to P(C630)
P(C634)_f	GTAGCCTATGCTAAGTGGGTGGAAGGGGACATG	68	33	QC to P(C634)
P(C634)_r	CATGTCCCTTCCACGCACTTAGCATAGGCTAC	68	33	QC to P(C634)
P(C638)_f	CTAAGAAAGTGGAAGGGTGCATGTACGAGTCTGCC	68	35	QC to P(C638)
P(C638)_r	GGCAGACTCGTACATGCACCCTTCCACTTCTTAG	68	35	QC to P(C638)
P(C642)_f	GGGGACATGTACGAGTGCGCCAACAGCAGGGATG	73	34	QC to P(C642)
P(C642)_r	CATCCCTGCTGTTGGCGCACTCGTACATGTCCCC	73	34	QC to P(C642)
P(C648)_f	GCCAACAGCAGGGATTGCTATTATCACTTATTAGCAG	65	37	QC to P(C648)
P(C648)_r	CTGCTAATAAGTGATAATAGCAATCCCTGCTGTTGGC	65	37	QC to P(C648)
pGEX-4T1_f	GTGCCTGGATGCGTTCCTCAAAATT	62	24	seq of pGEX-4T1
pGEX-4T1_r	CACCCGCTGACGCGCCCTGACGGG	73	24	seq of pGEX-4T1
P_f1	agtcggatccGGTGAAGGAAAGGCTGGCACG	71	32	R-L of P's into pGEX-4T5-GFP
P_r1	agtcctcatggtACGCGACCTCCGTTTTTCTTCTAG	68	35	R-L of P's into pGEX-4T5-GFP
Cherry_f	CTAGAAGAAAAACGGAGGTCGCGTACCATGGTGAGCAAGGGCGAGGAGG	75	49	<i>in vivo</i> cloning of Cherry into GEX-4T5-GFP
Cherry_r	CGCTCGAGTCGACCCGGGAATTCCTTGACAGCTCGTCCATGCCG	77	45	<i>in vivo</i> cloning of Cherry into GEX-4T5-GFP
pGEX-4T5_f	CCGGGAGCTGCATGTGTCAG			seq of pGEX-4T5
pGEX-4T5_r	GGCCTTTGCAGGGCTGGC			seq of pGEX-4T5
P_f2	GATGGAATTCACCATGGGTGAAGGAAAGGC	65	31	R-L of P's into YFP N1
P_r2	GATGGGATCCACACGCGACCTCC	67	23	R-L of P's into YFP N1
Cherry_f	ATCCACCGGTCGCCACCATGGTGAGC	70	26	R-L of Cherry into YFP N1
Cherry_r	AGTCGCGGCCGCTGGACTTGACAGCTCGTCCATGCCG	77	48	R-L of Cherry into YFP N1
pmCherry N1_f	CGCAAATGGGCGGTAGGCGTG	65	21	seq of pmCherry N1
pmCherry N1_r	GATGAGTTTGACAAACCAC	55	20	seq of pmCherry N1

Table S2: List of DNA- and aa-sequences of proteins **P** for expression in *E. coli*. A cloning artifact stemming from the TEV-cleavage of the GST-tag is highlighted in blue, introduced cysteine mutations are highlighted in yellow.

protein P:

DNA-sequence

GGCGCCATGGGTGTAAGGAAAGGCTGGCACGAACATGTCACCTCAGGACCTGCGGAGCCATCTAGTG
CATAAACTCGTCCAAGCCATCTTCCCAACACCTGATCCCGCAGCTCTAAAGGATCGCCGCATGGAAAA
CCTGGTAGCCTATGCTAAGAAAGTGGAAGGGGACATGTACGAGTCTGCCAACAGCAGGGATGAATATT
ATCACTTATTAGCAGAGAAAAATCTACAAGATACAAAAAGAACTAGAAGAAAAACGGAGGTCGCGT

amino acid sequence

GAMGVRKGWHEHVTQDLRSHLVHKLVAIFPTDPAALKDRRME
NLVAYAKKVEGDMYESANSRDEYYHLLAEKIYKIQKELEEKRRSR

protein P(E626C):

DNA-sequence

GGCGCCATGGGTGTAAGGAAAGGCTGGCACGAACATGTCACCTCAGGACCTGCGGAGCCATCTAGTG
CATAAACTCGTCCAAGCCATCTTCCCAACACCTGATCCCGCAGCTCTAAAGGATCGCCGCATGTGCAA
CCTGGTAGCCTATGCTAAGAAAGTGGAAGGGGACATGTACGAGTCTGCCAACAGCAGGGATGAATATT
ATCACTTATTAGCAGAGAAAAATCTACAAGATACAAAAAGAACTAGAAGAAAAACGGAGGTCGCGT

amino acid sequence

GAMGVRKGWHEHVTQDLRSHLVHKLVAIFPTDPAALKDRRMC
NLVAYAKKVEGDMYESANSRDEYYHLLAEKIYKIQKELEEKRRSR

protein P(A630C):

DNA-sequence

GGCGCCATGGGTGTAAGGAAAGGCTGGCACGAACATGTCACCTCAGGACCTGCGGAGCCATCTAGTG
CATAAACTCGTCCAAGCCATCTTCCCAACACCTGATCCCGCAGCTCTAAAGGATCGCCGCATGGAAAA
CCTGGTAGCCTATGCTAAGAAAGTGGAAGGGGACATGTACGAGTCTGCCAACAGCAGGGATGAATATT
ATCACTTATTAGCAGAGAAAAATCTACAAGATACAAAAAGAACTAGAAGAAAAACGGAGGTCGCGT

amino acid sequence

GAMGVRKGWHEHVTQDLRSHLVHKLVAIFPTDPAALKDRRMC
NLVYAKKVEGDMYESANSRDEYYHLLAEKIYKIQKELEEKRRSR

protein P(K634C):

DNA-sequence

GGCGCCATGGGTGTAAGGAAAGGCTGGCACGAACATGTCACCTCAGGACCTGCGGAGCCATCTAGTG
CATAAACTCGTCCAAGCCATCTTCCCAACACCTGATCCCGCAGCTCTAAAGGATCGCCGCATGGAAAA
CCTGGTAGCCTATGCTAAGTGGTGGAAGGGGACATGTACGAGTCTGCCAACAGCAGGGATGAATATT
ATCACTTATTAGCAGAGAAAAATCTACAAGATACAAAAAGAACTAGAAGAAAAACGGAGGTCGCGT

amino acid sequence

GAMGVRKGWHEHVTQDLRSHLVHKLVAIFPTDPAALKDRRME
NLVAYAKKVEGDMYESANSRDEYYHLLAEKIYKIQKELEEKRRSR

protein P(D638C):

DNA-sequence

GGCGCCATGGGTGTAAGGAAAGGCTGGCACGAACATGTCACCTCAGGACCTGCGGAGCCATCTAGTG
CATAAACTCGTCCAAGCCATCTTCCCAACACCTGATCCCGCAGCTCTAAAGGATCGCCGCATGGAAAA
CCTGGTAGCCTATGCTAAGTGGTGGAAGGGGACATGTACGAGTCTGCCAACAGCAGGGATGAATATT
ATCACTTATTAGCAGAGAAAAATCTACAAGATACAAAAAGAACTAGAAGAAAAACGGAGGTCGCGT

amino acid sequence

GAMGVRKGWHEHVTQDLRSHLVHKLVAIFPTDPAALKDRRME
NLVAYAKKVEGDMYESANSRDEYYHLLAEKIYKIQKELEEKRRSR

protein P(S642C):

DNA-sequence

GGCGCCATGGGTGTAAGGAAAGGCTGGCACGAACATGTCACCTCAGGACCTGCGGAGCCATCTAGTG
CATAAACTCGTCCAAGCCATCTTCCCAACACCTGATCCCGCAGCTCTAAAGGATCGCCGCATGGAAAA
CCTGGTAGCCTATGCTAAGAAAGTGGAAGGGGACATGTACGAGTGGGCCAACAGCAGGGATGAATATT
ATCACTTATTAGCAGAGAAAAATCTACAAGATACAAAAAGAACTAGAAGAAAAACGGAGGTCGCGT

amino acid sequence

GAMGVRKGWHEHVTQDLRSHLVHKLVAIFPTDPAALKDRRME
NLVAYAKKVEGDMYESANSRDEYYHLLAEKIYKIQKELEEKRRSR

protein P(E648C):

DNA-sequence

GGCGCCATGGGTGTAAGGAAAGGCTGGCACGAACATGTCACCTCAGGACCTGCGGAGCCATCTAGTG
CATAAACTCGTCCAAGCCATCTTCCCAACACCTGATCCCGCAGCTCTAAAGGATCGCCGCATGGAAAA
CCTGGTAGCCTATGCTAAGAAAGTGGAAGGGGACATGTACGAGTGGGCCAACAGCAGGGATGGCTATT
ATCACTTATTAGCAGAGAAAAATCTACAAGATACAAAAAGAACTAGAAGAAAAACGGAGGTCGCGT

amino acid sequence

GAMGVRKGWHEHVTQDLRSHLVHKLVAIFPTDPAALKDRRME
NLVAYAKKVEGDMYESANSRDEYYHLLAEKIYKIQKELEEKRRSR

Table S3: List of DNA- and aa-sequences of proteins **P** in conjugation with Cherry as they were expressed in HeLa and Hek293 cells. The introduced cysteine mutation in **P(C638)**-Cherry is highlighted in yellow.

protein P(wt)-Cherry:

DNA-sequence

ATGGGTGTAAGGAAAGGCTGGCACGAACATGTCACTCAGGACCTGCGGAGCCATCTAGTGCATAAAC
TCGTCCAAGCCATCTTCCCAACACCTGATCCCGCAGCTCTAAAGGATCGCCGCATGGAAAACCTGGTA
GCCTATGCTAAGAAAGTGGAAGGGGACATGTACGAGTCTGCCAACAGCAGGGATGAATATTATCACTTA
TTAGCAGAGAAAAATCTACAAGATACAAAAAGAACTAGAAGAAAAACGGAGGTCGCGTGGGGATCCACC
GGTCGCCACCATGGTGAGCAAGGGCGAGGAGGATAACATGGCCATCATCAAGGAGTTCATGCGCTTC
AAGGTGCACATGGAGGGCTCCGTGAACGGCCACGAGTTCGAGATCGAGGGCGAGGGCGAGGGCCG
CCCCTACGAGGGCACCCAGACCGCCAAGCTGAAGGTGACCAAGGGTGGCCCCCTGCCCTTCGCCTG
GGACATCCTGTCCCCTCAGTTCATGTACGGCTCCAAGGCCCTACGTGAAGCACCCCGCCGACATCCCC
GACTACTTGAAAGCTGTCTTCCCGAGGGCTTCAAGTGGGAGCGCGTGATGAACCTCGAGGACGGCG
GCGTGGTGACCGTGACCCAGGACTCCTCCCTGCAGGACGGCGAGTTCATCTACAAGGTGAAGCTGCG
CGGCACCAACTTCCCCTCCGACGGCCCCGTAATGCAGAAGAAGACCATGGGCTGGGAGGCCTCCTCC
GAGCGGATGTACCCCGAGGACGGCGCCCTGAAGGGCGAGATCAAGCAGAGGCTGAAGCTGAAGGAC
GGCGGCCACTACGACGCTGAGGTCAAGACCACCTACAAGGCCAAGAAGCCCGTGCAGCTGCCCGGC
GCCTACAACGTCAACATCAAGTTGGACATCACCTCCCAACAGGAGCTACACCATCGTGGAAACAGTAC
GAACGCGCCGAGGGCCGCCACTCCACCGCGGCATGGACGAGCTGTACAAGTAG

amino acid sequence

MGVRKGWHEHVTQDLRSHLVHKLVAIFPTDPAALKDRRMENLVAYAKKVEGDMYESANSRDEYYHLLA
EKIYKIQKELEEKRRSRGDPVATMVSKGEEDNMAIIEFMRFKVHMEGSVNGHEFEIEGEGEGRPYEGTQ
TAKLKVTGKGPLPFAWDILSPQFMYGSKAYVKHPADIPDYLKLSFPEGFKWERVMNFEDGGVVTVTQDSSL
QDGEFIYVKLRGTNFPDGPVMQKKTMGWEASSERMYPEDGALKGEIKQLRLKLDGGHYDAEVKTTYK
AKKPVQLPGAYNVNLIKLDITSHNEDYTIVEQYERAEGRHSTGGMDLYK

protein P(C638)-Cherry:

DNA-sequence

ATGGGTGTAAGGAAAGGCTGGCACGAACATGTCACTCAGGACCTGCGGAGCCATCTAGTGCATAAAC
TCGTCCAAGCCATCTTCCCAACACCTGATCCCGCAGCTCTAAAGGATCGCCGCATGGAAAACCTGGTA
GCCTATGCTAAGAAAGTGGAAGGGTGCATGTACGAGTCTGCCAACAGCAGGGATGAATATTATCACTTA
TTAGCAGAGAAAAATCTACAAGATACAAAAAGAACTAGAAGAAAAACGGAGGTCGCGTGGGGATCCACC
GGTCGCCACCATGGTGAGCAAGGGCGAGGAGGATAACATGGCCATCATCAAGGAGTTCATGCGCTTC
AAGGTGCACATGGAGGGCTCCGTGAACGGCCACGAGTTCGAGATCGAGGGCGAGGGCGAGGGCCG
CCCCTACGAGGGCACCCAGACCGCCAAGCTGAAGGTGACCAAGGGTGGCCCCCTGCCCTTCGCCTG
GGACATCCTGTCCCCTCAGTTCATGTACGGCTCCAAGGCCCTACGTGAAGCACCCCGCCGACATCCCC
GACTACTTGAAAGCTGTCTTCCCGAGGGCTTCAAGTGGGAGCGCGTGATGAACCTCGAGGACGGCG
GCGTGGTGACCGTGACCCAGGACTCCTCCCTGCAGGACGGCGAGTTCATCTACAAGGTGAAGCTGCG
CGGCACCAACTTCCCCTCCGACGGCCCCGTAATGCAGAAGAAGACCATGGGCTGGGAGGCCTCCTCC
GAGCGGATGTACCCCGAGGACGGCGCCCTGAAGGGCGAGATCAAGCAGAGGCTGAAGCTGAAGGAC
GGCGGCCACTACGACGCTGAGGTCAAGACCACCTACAAGGCCAAGAAGCCCGTGCAGCTGCCCGGC
GCCTACAACGTCAACATCAAGTTGGACATCACCTCCCAACAGGAGCTACACCATCGTGGAAACAGTAC
GAACGCGCCGAGGGCCGCCACTCCACCGCGGCATGGACGAGCTGTACAAGTAG

amino acid sequence

MGVRKGWHEHVTQDLRSHLVHKLVAIFPTDPAALKDRRMENLVAYAKKVEGMYESANSRDEYYHLLA
EKIYKIQKELEEKRRSRGDPVATMVSKGEEDNMAIIEFMRFKVHMEGSVNGHEFEIEGEGEGRPYEGTQ
TAKLKVTGKGPLPFAWDILSPQFMYGSKAYVKHPADIPDYLKLSFPEGFKWERVMNFEDGGVVTVTQDSSL
QDGEFIYVKLRGTNFPDGPVMQKKTMGWEASSERMYPEDGALKGEIKQLRLKLDGGHYDAEVKTTYK
AKKPVQLPGAYNVNLIKLDITSHNEDYTIVEQYERAEGRHSTGGMDLYK

Table S 4: List of DNA- and aa-sequences of proteins **P** in conjugation with Cherry as they were expressed in *E. coli* cells. The introduced cysteine mutation in **P(C638)**-Cherry is highlighted in yellow.

protein P(WT)-Cherry:

DNA-sequence

CGTGTAAAGGAAAGGCTGGCAGCAACATGTCACTCAGGACCTGCGGAGCCATCTAGTGCATAAACTCGTCCAAGCCATCTTCCCAACACC
TGATCCCGCAGCTCTAAAGGATCGCCGCATGGAAAACCTGGTAGCCTATGCTAAGAAAGTGGAAGGGGACATGTACGAGTCTGCCAACA
GCAGGGATGAATATTATCACTTATTAGCAGAGAAAATCTACAAGATACAAAAGAACTAGAAGAAAAACGGAGGTCGCGTACCATGGTGAG
CAAGGGCGAGGAGGATAACATGGCCATCATCAAGGAGTTTCATGCGCTTCAAGGTGCACATGGAGGGCTCCGTGAACGGCCACGAGTTT
GAGATCGAGGGCGAGGGCGAGGGCCGCCCTACGAGGGCACCCAGACCGCCAAGCTGAAGGTGACCAAGGGTGGCCCCCTGCCCTT
CGCCTGGGACATCCTGTCCCTCAGTTTCATGTACGGCTCCAAGGCCTACGTGAAGCACCCCGCCGACATCCCCGACTACTTGAAGCTGT
CCTTCCCGAGGGCTTCAAGTGGGAGCGCGTGATGAACTTCGAGGACGGCGCGCTGGTGACCGTGACCCAGGACTCCTCCCTGCAGG
ACGGCGAGTTTCATCTACAAGGTGAAGCTGCGCGGCACCAACTTCCCTCCGACGGCCCCGTAATGCAGAAGAAGACCATGGGCTGGGA
GGCCTCCTCCGAGCGGATGTACCCCGAGGACGGCGCCCTGAAGGGCGAGATCAAGCAGAGGCTGAAGCTGAAGGACGGCGGCCACTA
CGACGCTGAGGTCAAGACCACCTACAAGGCCAAGAAGCCCGTGCAGCTGCCCGGCCCTACAACGTCAACATCAAGTTGGACATCACC
TCCACAACGAGGACTACACCATCGTGGAACAGTACGAACGCGCCGAGGGCCGCCACTCCACCGGCGGCATGGACGAGCTGTACAAG
GAATCCCGGGTCTGACTCGAGCGGCCGCATCGTACTGA

aa-sequence

VRKGWHEHVTQDLRSHLVHKLVAIFPTPDPAALKDRRMENLVAYAKKVEGDMYESANSRDEYYHLLAEKIYKIQKELEEKRRSRMTMVSKE
EDNMAIIEFMRFKVHMEGVSNGHEFEIEGEGEGRPYEGTQTAKLVTKGGPLPFAWDILSPQFMYGSKAYVKHPADIPDYLKLSFPEGFKWE
RVMNFEDGGVVTVTQDSSLQDGEFIYKVLKRGTFNPSDGPVMQKKTMGWEASSERMYPEDGALKGEIKQRLKLDGGHYDAEVKTTYKAKK
PVQLPGAYNVNLIKLDITSHNEDYTIVEQYERAEGRHSTGGMDLYKEFPGRRLRPHRD

protein P(C638)-Cherry:

DNA-sequence

CGTGTAAAGGAAAGGCTGGCAGCAACATGTCACTCAGGACCTGCGGAGCCATCTAGTGCATAAACTCGTCCAAGCCATCTTCCCAACACC
TGATCCCGCAGCTCTAAAGGATCGCCGCATGGAAAACCTGGTAGCCTATGCTAAGAAAGTGGAAGGGTGCATGTACGAGTCTGCCAACA
GCAGGGATGAATATTATCACTTATTAGCAGAGAAAATCTACAAGATACAAAAGAACTAGAAGAAAAACGGAGGTCGCGTACCATGGTGAG
CAAGGGCGAGGAGGATAACATGGCCATCATCAAGGAGTTTCATGCGCTTCAAGGTGCACATGGAGGGCTCCGTGAACGGCCACGAGTTT
GAGATCGAGGGCGAGGGCGAGGGCCGCCCTACGAGGGCACCCAGACCGCCAAGCTGAAGGTGACCAAGGGTGGCCCCCTGCCCTT
CGCCTGGGACATCCTGTCCCTCAGTTTCATGTACGGCTCCAAGGCCTACGTGAAGCACCCCGCCGACATCCCCGACTACTTGAAGCTGT
CCTTCCCGAGGGCTTCAAGTGGGAGCGCGTGATGAACTTCGAGGACGGCGCGCTGGTGACCGTGACCCAGGACTCCTCCCTGCAGG
ACGGCGAGTTTCATCTACAAGGTGAAGCTGCGCGGCACCAACTTCCCTCCGACGGCCCCGTAATGCAGAAGAAGACCATGGGCTGGGA
GGCCTCCTCCGAGCGGATGTACCCCGAGGACGGCGCCCTGAAGGGCGAGATCAAGCAGAGGCTGAAGCTGAAGGACGGCGGCCACTA
CGACGCTGAGGTCAAGACCACCTACAAGGCCAAGAAGCCCGTGCAGCTGCCCGGCCCTACAACGTCAACATCAAGTTGGACATCACC
TCCACAACGAGGACTACACCATCGTGGAACAGTACGAACGCGCCGAGGGCCGCCACTCCACCGGCGGCATGGACGAGCTGTACAAG
GAATCCCGGGTCTGACTCGAGCGGCCGCATCGTACTGA

aa-sequence

VRKGWHEHVTQDLRSHLVHKLVAIFPTPDPAALKDRRMENLVAYAKKVEGDMYESANSRDEYYHLLAEKIYKIQKELEEKRRSRMTMVSKE
EDNMAIIEFMRFKVHMEGVSNGHEFEIEGEGEGRPYEGTQTAKLVTKGGPLPFAWDILSPQFMYGSKAYVKHPADIPDYLKLSFPEGFKWE
RVMNFEDGGVVTVTQDSSLQDGEFIYKVLKRGTFNPSDGPVMQKKTMGWEASSERMYPEDGALKGEIKQRLKLDGGHYDAEVKTTYKAKK
PVQLPGAYNVNLIKLDITSHNEDYTIVEQYERAEGRHSTGGMDLYKEFPGRRLRPHRD

Table S5: List of proteins **P** including their molecular weight (MW), their isoelectric point (pI), their extinction coefficient (ϵ), their yield from a 2.5L TB-culture (see protein cloning & expression for details) and the distance from the introduced cysteine to the *N*-terminus of the ligand **L** are given for each protein. (a) **P**-Cherry fusion proteins expressed in human cell lines (b) **P**-Cherry fusion proteins expressed in *E. coli*.

protein	MW / Da	pI	ϵ / L·mol ⁻¹ ·cm ⁻¹	yield / mg	mean distance to <i>N</i> -terminus of ligand / Å
P(wt)	10477.9	9.22	12950	61	-
P(C626)	10452.0	9.30	12950	1.6	22
P(C630)	10510.0	9.07	12950	28	17
P(C634)	10452.9	8.75	12950	17	13
P(C638)	10466.0	9.30	12950	35	12
P(C642)	10494.0	9.07	12950	24	15
P(C648)	10452.0	9.30	12950	28	17
P(wt)-Cherry (a)	37691.7	6.29	47330	-	-
P(C638)-Cherry (a)	37679.7	6.44	47330	-	12
P(wt)-Cherry (b)	38514.58	6.51	47330	16	-
P(C638)-Cherry (b)	38502.63	6.70	47330	18	12

Table S6: List of peptides including their sequence, molecular formula (MF), molecular weight (MW), synthesis scale, yield, purity and analytical data from high-resolution mass spectrometry (MS; charge: no comment=+2, b=+3, c=+4. H = acetylated, f = fluorescein isothiocyanate, Cl = modified with α -chloroacetic acid, β Ala = beta-Alanine, PEG = polyethylene-glycol, bt = modified with Biotin, palm = modified with palmitic acid.

peptide	sequence	MF	MW / g·mol ⁻¹	scale / μmol	yield / %	purity / %	HRMS (a)	
							calculated	found
H-L-f	H-ILPSDIBDFVLKNTPS-WK(f)-CONH ₂	C ₁₂₂ H ₁₇₀ N ₂₄ O ₃₂ S	2516.8980	5.2	19	99	1258.61396	1258.61595
H-iL-f	H-SPTNKLVFDBIDSPLI-WK(f)-CONH ₂	C ₁₂₂ H ₁₇₀ N ₂₄ O ₃₂ S	2516.8980	2.0	6	84	1258.61396	1258.61523
Cl-4L-f	Cl-βAla-ILPSDIBDFVLKNTPS-WK(f)-CONH ₂	C ₁₂₅ H ₁₇₄ ClN ₂₅ O ₃₃ S	2622.4190	10.0	13	100	1311.11303	1311.11635
Cl-9L-f	Cl-PEG2-ILPSDIBDFVLKNTPS-WK(f)-CONH ₂	C ₁₂₈ H ₁₈₀ ClN ₂₅ O ₃₅ S	2696.4980	19.9	13	100	1348.13142	1348.13686
Cl-13L-f	Cl-PEG3-ILPSDIBDFVLKNTPS-WK(f)-CONH ₂	C ₁₃₁ H ₁₈₆ ClN ₂₅ O ₃₆ S	2754.5780	9.9	14	100	1377.15235	1377.15730
Cl-19L-f	Cl-PEG5-ILPSDIBDFVLKNTPS-WK(f)-CONH ₂	C ₁₃₅ H ₁₉₄ ClN ₂₅ O ₃₈ S	2842.6840	10.4	4	100	1421.17857	1421.18378
Cl-38L-f	Cl-(PEG5) ₂ -ILPSDIBDFVLKNTPS-WK(f)-CONH ₂	C ₁₄₈ H ₂₁₉ ClN ₂₆ O ₄₄ S	3134.0280	9.6	7	100	1044.51089 (b)	1044.50826 (b)
Cl-9iL-f	Cl-PEG2-SPTNKLVFDBIDSPLI-WK(f)-CONH ₂	C ₁₂₈ H ₁₈₀ ClN ₂₅ O ₃₅ S	2696.4980	10.5	5	100	1348.13142	1348.12256
Cl-9L-bt	Cl-PEG2-ILPSDIBDFVLKNTPS-WK[(PEG4) ₂ -bt]-CONH ₂	C ₁₃₉ H ₂₂₅ ClN ₂₈ O ₄₂ S	3027.9930	10.5	22	100	1513.79430	1513.79562
H-9L-bt	H-PEG2-ILPSDIBDFVLKNTPS-WK[(PEG4) ₂ -bt]-CONH ₂	C ₁₃₉ H ₂₂₆ N ₂₈ O ₄₂ S	2993.5510	9.7	27	100	1496.81378	1496.80565
Cl-9iL-bt	Cl-PEG2-SPTNKLVFDBIDSPLI-WK[(PEG4) ₂ -bt]-CONH ₂	C ₁₃₉ H ₂₂₅ ClN ₂₈ O ₄₂ S	3027.9930	16.5	11	100	1513.79430	1513.79501
f-MA	f-PEG2-KKKKKKSK(palm)-CONH ₂	C ₈₈ H ₁₄₄ N ₁₈ O ₁₈ S	1774.2880	3.1	20	100	592.02817 (b)	592.02741 (b)
Cl-9L-MA	Cl-PEG2-ILPSDIBDFVLKNTPS-W-PEG2-KKKKKKSK(palm)-CONH ₂	C ₁₆₉ H ₂₈₈ ClN ₃₇ O ₄₂	3545.8300	21.0	1	88	887.03674 (c)	887.03804 (c)
Cl-9iL-MA	Cl-PEG2-SPTNKLVFDBIDSPLI-W-PEG2-KKKKKKSK(palm)-CONH ₂	C ₁₆₉ H ₂₈₈ ClN ₃₇ O ₄₂	3545.8300	20.0	2	87	887.03674 (c)	887.03686 (c)
Y-9L-f	Y-PEG2-ILPSDIBDFVLKNTPS-WK(f)-CONH ₂	C ₁₃₂ H ₁₈₈ N ₂₆ O ₃₅ S	2731.1630	10.0	1	75	1366.18151	1366.18283

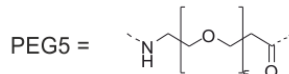
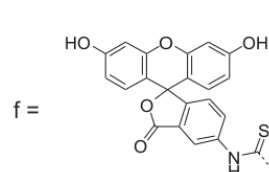
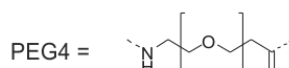
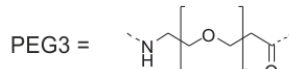
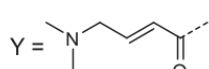
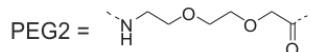
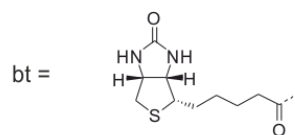


Table S7: Yield of the initial reaction tests of six proteins **P** against all five ligands **L**.

	time / h	Cl-4L-f		Cl-9L-f		Cl-13L-f		Cl-19L-f		Cl-38L-f	
		1	6	1	6	1	6	1	6	1	6
P(C626)		-	9	-	27	-	20	-	28	6	37
P(C630)		-	21	5	53	27	85	62	98	27	61
P(C634)		18	84	58	100	47	97	51	95	18	56
P(C638)		39	90	100	99	100	100	100	100	69	73
P(C642)		-	-	-	2	-	30	3	60	-	20
P(C648)		-	37	6	59	5	55	40	93	54	72

Table S8: Initial reaction rates of the ligation reactions between six proteins **P** and all five ligands **L**.

	initial reaction rates / nM·s ⁻¹				
	Cl-4L-f	Cl-9L-f	Cl-13L-f	Cl-19L-f	Cl-38L-f
P(C626)	0.041	0.12	0.094	0.13	0.16
P(C630)	0.10	0.15	0.75	1.7	0.75
P(C634)	0.49	1.6	1.3	1.4	0.49
P(C638)	1.1	> 2.8	> 2.8	> 2.8	1.9
P(C642)	-	0.010	0.14	0.073	0.093
P(C648)	0.17	0.16	0.12	1.1	1.5

Table S9: Probability of occurrence (*P*) of the reacting atoms (cysteinic sulfur and α carbon of α chloroacetamide) within a distance of 5 Å. Data obtained from 500 ns MD simulations using AMBER14.

	probability for distance < 5Å between S of P and αC of L				
	Cl-4L-f	Cl-9L-f	Cl-13L-f	Cl-19L-f	Cl-38L-f
P(C626)	0	0	0	0.6	4.1
P(C630)	0.2	0.8	2.4	4.4	6.3
P(C634)	4.6	17	6.7	11	11
P(C638)	19	15	16	13	11
P(C642)	0	1.3	4.2	4.0	2.2
P(C648)	0	0	0.2	1.5	0

Table S10: Yields of ligation reactions based on three independent measurements for protein **P(C638)** with the ligands **CI-9/13/19L-f** and ligand **CI-9iL-f** as well as for different GSH concentrations with ligand **CI-9L-f**. We estimated the detection limit of our HPLC to be 2%. Although yields above 30% were detected, we did not take them into account for the calculation (numbers in brackets).

	time / min	yield / %				time / min	yield / %		
		value 1	value 2	value 3			value 1	value 2	value 3
P(C638) + CI-9L-f	0.5	-	-	-	P(C638) + CI-9iL-f	0.5	-	-	-
	1.0	12	2	6		1.0	-	-	-
	1.5	25	13	10		1.5	-	-	-
	2.0	31	32	19		2.0	-	-	-
	2.5	39	37	31		2.5	-	-	-
	5.0	(63)	(54)	(42)		5.0	-	-	-
	10.0	(84)	(87)	(74)		10.0	-	-	-
	15.0	(100)	(95)	(85)		15.0	-	-	-
	30.0	(100)	(100)	(89)		30.0	-	5	5
	60.0	(100)	(100)	(100)		60.0	6	7	3
	120.0	(100)	(100)	(100)		120.0	17	5	8
	180.0	(100)	(100)	(100)		180.0	25	22	13
	360.0	(100)	(100)	(100)		360.0	(55)	(44)	(26)
	540.0	(100)	(100)	(100)		540.0	(68)	(63)	(38)
	720.0	(100)	(100)	(100)		720.0	(78)	(63)	(47)
P(C638) + CI-13L-f	0.5	-	-	-	5 mM GSH + CI-9L-f	0.5	-	-	-
	1.0	-	-	-		1.0	-	-	-
	1.5	10	-	4		1.5	-	-	-
	2.0	13	4	8		2.0	-	-	-
	2.5	19	6	11		2.5	-	-	-
	5.0	38	16	22		5.0	-	-	-
	10.0	(64)	(41)	(45)		10.0	-	-	-
	15.0	(93)	(59)	(59)		15.0	-	-	-
	30.0	(96)	(85)	(91)		30.0	-	-	-
	60.0	(100)	(94)	(99)		60.0	-	4	-
	120.0	(100)	(100)	(99)		120.0	-	10	5
	180.0	(100)	(100)	(100)		180.0	16	17	12
	360.0	(100)	(100)	(100)		360.0	(39)	(39)	25
	540.0	(100)	(100)	(100)		540.0	(46)	(53)	(35)
	720.0	(100)	(100)	(100)		720.0	(55)	(64)	(51)
P(C638) + CI-19L-f	0.5	-	-	-	20 μ M GSH + CI-9L-f	0.5	-	-	-
	1.0	7	-	-		1.0	-	-	-
	1.5	15	-	7		1.5	-	-	-
	2.0	20	9	10		2.0	-	-	-
	2.5	24	15	13		2.5	-	-	-
	5.0	(43)	29	29		5.0	-	-	-
	10.0	(66)	(55)	(49)		10.0	-	-	-
	15.0	(72)	(74)	(67)		15.0	-	-	-
	30.0	(96)	(94)	(94)		30.0	-	-	-
	60.0	(100)	(99)	(99)		60.0	-	-	-
	120.0	(100)	(100)	(100)		120.0	-	-	-
	180.0	(100)	(100)	(100)		180.0	-	-	-
	360.0	(100)	(100)	(100)		360.0	2	-	2
	540.0	(100)	(100)	(100)		540.0	3	-	3
	720.0	(100)	(100)	(100)		720.0	6	3	2

3 SI METHODS

1.1 Protein cloning, expression & purification

The sequence for the wildtype KIX domain **P(wt)** was obtained in a modified pGEX-4T1 vector. To obtain the six single cysteine variants, this vector was modified via quick change protocol (see Table S1 for primer sequences and properties, Table S3 for protein sequences and Table S5 for protein parameters). Obtained vectors were sequenced at StarSEQ® GmbH (Mainz, Germany) to ensure correctness.

All proteins were expressed in *E. coli* as GST fusion proteins according to the following protocol: A transformation of *E. coli* BL21 DE3 was performed and after incubation on an ampicillin plate (100 µg/mL ampicillin) at 37°C over night a 2.5 L culture of terrific broth medium containing 100 µg/mL ampicillin was inoculated by rinsing the plate. The cultures were grown until OD₆₀₀ reached 0.6 – 0.8. Afterwards the expression was induced with a 1 mM IPTG stock (final concentration 0.2 mM IPTG) and performed at 18°C. After approximately 15 h the cultures were harvested by centrifugation at 4000 rcf and 4°C for 10 min. The cellular pellets were resuspended in 30 mL lysis buffer (500 mM NaCl, 50 mM HEPES pH 7.4, 2 mM TCEP) and either stored at -80°C or directly processed for protein purification.

For purification of proteins the corresponding pellet was thawed at 37°C (if necessary) and the final lysate volume was adjusted to 100 mL with lysis buffer. DNase was added and the concentration of PMSF was adjusted to 2 mM with a 200 mM stock solution in ethanol. The pellet was resolved with a disperser (T18 Ultra turrax from IKA®-Werke GmbH & Co. KG, Staufen, Germany) and cells were disrupted with a high-pressure homogenizer (Microfluidizer® 1109 from Microfluidics Corporation, Westwood, USA). Thereafter, the lysate was centrifuged at 70.000 rcf and 4°C for 1 h to separate the cellular debris. The supernatant was applied to a 30 mL column packed with Glutathione Sepharose High Performance (GE Healthcare Europe GmbH, Freiburg, Germany) equilibrated with lysis buffer to isolate the GST-fusion protein. After washing with 300 mL lysis buffer and 150 mL gel filtration buffer (100 mM NaCl, 50 mM HEPES pH 7.4, 2 mM TCEP) the protein of interest was eluted with 50 mL elution buffer (100 mM NaCl, 50 mM HEPES pH 7.4, 2 mM TCEP, 20 mM GSH). Fractions of 5 mL were collected and all fractions with a protein concentration above 0.01 mg/mL (as determined with UV/Vis-measurement at 210 nm) were combined. TEV-protease was added and the solution was incubated at 4°C over night to remove the GST-tag. For final protein purification the solution was applied to a gel filtration column (HiLoad 16/600 Superdex 75 pg from GE Healthcare Europe GmbH, Freiburg, Germany). If necessary remaining GST was removed using a 5 mL GSTrap FF column (GE Healthcare Europe GmbH, Freiburg, Germany). Purified proteins were concentrated via ultracentrifugation and stored at -80°C. For a comparative SDS-PAGE of all seven protein variants see Figure S1. To ensure correct mutation all protein variants were subjected to HPLC-MS analysis. See Figure S2-8 for representative chromatograms and MS spectra.

1.2 Peptide synthesis

Peptide synthesis was performed via manual solid-phase peptide synthesis according to Fmoc-based protocols. For all derivatives of **L** and **iL** a Rink Amide MBHA resin (100 – 200 mesh) from Iris Biotech GmbH (Marktredwitz, Deutschland) was used. For peptides with nuclear membrane anchor (**f-MA**, **9L-MA** and **9iL-MA**) NovaSyn®TGR resin (Merck KGaA, Darmstadt, Germany) was used.

All coupling steps were performed with 4 eq Fmoc-protected amino acids, 4 eq coupling reagent(s) and 8 eq base in DMF while shaking at room temperature. All couplings were performed twice with COMU/Oxyma and DIPEA for 30 min in the first coupling and with PyBOP and NMM for 2 h in the second coupling. After each double coupling, Kaiser's test was performed and if necessary the double coupling was repeated. If coupling efficiency was satisfying a capping step with acetic anhydride and DIPEA in DMF ($\text{Ac}_2\text{O}/\text{DIPEA}/\text{DMF} = 1:1:10$) was performed for 5 min at room temperature. Thereafter, the *N*-terminal Fmoc-group was removed with 25% piperidin in DMF (2x 5 min).

For *C*-terminal modification Fmoc-Lys(Mmt)-OH was introduced as first amino acid on the resin. After synthesis of the complete peptide including spacers the Mmt-group was cleaved by washing with TFA/TIPS/DCM (2:5:94) until the solution was colorless. Further modification with fluorophore **f** was performed at room temperature for 2x 2 h with 4 eq FITC and 8 eq DIPEA. For modification with **bt** the Mmt group was removed and afterwards a standard double coupling was performed with Mmt-PEG₄-OH. After Kaiser's test and capping, the Mmt-group was deprotected and another coupling with Mmt-PEG₄-OH was performed. Finally, the Mmt was deprotected and a double coupling with Biotin (4 eq), PyBOP (4 eq) and DIPEA (8 eq) was performed in DMF for 1 h each.

For introduction of the electrophilic α -chloroacetamide group the *N*-terminal Fmoc- group of the PEG-spacer was removed as described above. Thereafter, double coupling of α -chloroacetic acid (5 eq) was performed with 5 eq PyBOP and 12 eq DIPEA for 2x 1 h at room temperature in DMF. For unreactive peptide **H-9L** the last Fmoc-group was removed and a standard capping step was performed to acetylate the peptide.

Final cleavage of the resin was performed with TFA/H₂O/EDT/TIPS (94:2.5:2.5:1) at room temperature for 3 h while shaking. Thereafter, the resin was washed shortly with cleavage solution. The combined solutions were concentrated by evaporation to 0.5 mL, the peptide was precipitated with Et₂O (14 mL, -20°C) and pelleted by centrifugation for 15 min at 4°C and 3000 rcf. After removal of the supernatant, the pellet was dried and resolved in ACN/H₂O. All peptides were purified with preparative reversed-phase HPLC. Depending on peptide amount either a Nucleodur C18 reverse-phase column (10x50 mm, 110 Å, particle size 5 µm, MACHEREY-NAGEL GmbH & Co. KG, Düren, Germany, flow rate 6 mL · min⁻¹) or a Nucleodur C18 reverse-phase column (10x125 mm, 110 Å, particle size 5 µm, MACHEREY-NAGEL GmbH & Co. KG, Düren, Germany, flow rate 17.5 mL · min⁻¹) was used. According to

the peptide properties different gradients were used (solvent A: H₂O with 0.1% TFA, solvent B: ACN with 0.1% TFA). Obtained fractions were analyzed via HPLC-MS (1200 system equipped with a Zorbax Eclipse, XDB-C18 reverse-phase column 4.6x150 mm, particle size 5 µm from Agilent Technologies, Santa Clara, California, USA coupled with a LCQ Advantage Max (Finnigan™) from Thermo Scientific, Waltham, Massachusetts, USA) and pooled regarding their purity.

Yields were determined with the absorption of **f** if possible. Therefore a small volume of pooled fractions was added to 100 mM sodium phosphate buffer (pH 8.5) and the absorption at 494 nm was measured using a V-550 UV/VIS spectrophotometer (Jasco, Easton, Maryland, USA). For calculation an extinction coefficient of $\epsilon = 77.000 \text{ L}\cdot\text{mol}^{-1}\cdot\text{cm}^{-1}$ was used. For peptides without **f**-modification the extinction coefficient at 280 nm from the contained tryptophane was calculated to be $\epsilon = 5.500 \text{ L}\cdot\text{mol}^{-1}\cdot\text{cm}^{-1}$ using ProtParam.² A summary of peptide sequences, modifications and parameters is listed in Table S6.

1.3 Fluorescence polarization (FP) assay

For FP assay peptide ligands **L** and **iL** were *N*-terminally capped and *C*-terminally modified with **f**. All peptides were used as 20 µM DMSO-stock solutions and diluted to 50 nM with FP-buffer (100 mM NaCl, 50 mM HEPES pH 7.4, 0.1% Tween-20). All proteins were obtained in gelfiltration buffer (100 mM NaCl, 50 mM HEPES pH 7.4, 2 mM TCEP) and diluted to 0.1 mM with FP-buffer. In a 384-well plate (384 Well Low Volume Black Round Bottom Polystyrene NBS™ Microplate from Corning, GmbH, Wiesbaden, Germany) the proteins were provided in a dilution series ranging from 40 µM to 26.8 nM with dilution steps of 2.5. To each well the 50 nM peptide solution was added to obtain a final peptide concentration of 20 nM. After a short centrifugation step the plate was incubated for 1 h at room temperature before measuring fluorescence polarization using a Safire2™ plate reader (Tecan Group Ltd, Männedorf, Switzerland). Settings were $\lambda_{\text{ex}} = 485 \text{ nm}$ and $\lambda_{\text{em}} = 525 \text{ nm}$. To obtain the dissociation constants the raw data was processed using GraphPad Prism 5.0 for Windows (GraphPad Software, San Diego, California, USA). The mean value and the SD of triplicate measurements were transformed to a logarithmic scale and analyzed using the non-linear regression method log(agonist) vs. response. In Figure S9 and S10 the data including K_D -values are shown.

1.4 Initial reactivity tests

For initial tests all six protein **P** variants were incubated with all five ligands **Cl-nL-f** at 37°C for 1 h and 6 h, respectively. Therefore, 1 mM stock solutions of each ligand in DMSO as well as 1 mM stock solutions of each protein in gel filtration buffer (100 mM NaCl, 50 mM HEPES pH 7.4, 2 mM TCEP) were prepared. Peptide stocks were further diluted with buffer (100 mM NaCl, 50 mM HEPES pH 7.4) to 20 µM. Proteins were further diluted with the same buffer to 40 µM. Equal amounts (25 µL) of these

peptide and protein containing solutions were combined and incubated at 37°C for 1 h and 6 h in reaction tubes (Safe-Lock Tubes, 1.5 mL from Eppendorf, Wesseling-Berzdorf, Germany). After incubation, reaction mixtures were quenched by addition of 0.5 μ L TFA (final concentration 1%) and readout was performed via reversed-phase HPLC separation of the reaction mixture (Hitachi HPLC LaChrom Elite Serie system from Hitachi, Tokyo, Japan equipped with a Zorbax Eclipse, XDB-C18 reverse-phase column 4.6x150 mm, particle size 5 μ m from Agilent Technologies, Santa Clara, California, USA ; solvent A: H₂O with 0.1% TFA, solvent B: ACN with 0.1% TFA, gradient: 30-95% B in 10 min) coupled with UV/Vis-detection at 210 nm and 440 nm. An exemplary chromatogram is shown in Figure S11, the measured yields in percentage are listed in Table S7 and initial reaction rates are listed in Table S8. For data processing see section 1.7.

1.5 Molecular dynamics (MD) simulations

1.5.1 Structure preparation

The basis of the MD simulations was provided by the NMR structure of the complex between the KIX domain of CBP (residues 586-672) and the TAD of MLL (residues 842-858) with PDB ID 2LXS.³ The residue numbering is given according to this PDB structure. From the ensemble of 20 NMR models we selected the first one as starting point for MD simulations. The structures of TAD and KIX were prepared using Maestro.⁴ Missing amino acids S859 and W860 were added to the C-terminus of TAD and amino acids 840-843 were removed from its N-terminus. The 3D structures of the linkers were built manually and connected to the backbone of TAD via the free N-terminus of amino acid I844. The different single cysteine variations were manually added to the KIX domain.

1.5.2 MD simulations

All MD simulations were conducted with AMBER14 on GPU using Sander for minimization and equilibration, and PMEMD for the production runs.⁵⁻⁷ In total, thirty MD simulations were performed in explicit water using the six single cysteine variants of KIX (C626, C630, C634, C638, C642, C648) and five different TAD-bound linkers (4L, 9L, 13L, 19L, 38L) resulting in overall simulation times of 3 μ s for the conventional MD (cMD) simulations and 15 μ s for the accelerated MD (aMD) simulations. Force field parameters for the linkers were taken from the general AMBER forcefield (GAFF).⁸ Atomic charges for the linkers were determined by the restraint electrostatic potential (RESP) fit procedure using Gaussian09 and Antechamber.⁹⁻¹¹ Protein atoms and structurally bound ions were described by the ff14SB forcefield.^{12,13} The protein/peptide complexes were generated with LEaP. Each complex was placed in an octahedral TIP3P water box with an extension of at least 11 Å in each direction from the solute and neutralized by adding Na⁺ or Cl⁻ counter ions.¹⁴ Solvated systems were then subjected to a two-step minimization procedure to remove clashes between the water molecules and the solute: (1)

50 steps of steepest descent and 200 steps of conjugate gradient minimization with harmonic positional restraints of strength $25 \text{ kcal}\cdot\text{mol}^{-1}\cdot\text{\AA}^{-2}$ on all solute atoms, (2) 50 steps of steepest descent and 200 steps of conjugate gradient minimization with harmonic positional restraints of strength $5 \text{ mol}^{-1}\cdot\text{\AA}^{-2}$ on all solute atoms. After minimization, four steps of equilibration were run: (1) 50 ps NVT simulation to increase the thermostat target temperature from 100 K to 300 K using Berendsen's temperature and pressure control algorithms with time constants of 0.5 ps for both heat bath coupling and pressure relaxation, (2) 50 ps NPT simulation at constant isotropic pressure of 1 atm to adjust the density of the system to $1 \text{ g}\cdot\text{cm}^{-3}$, (3) five 50 ps NVT simulations progressively decreasing the restraints in steps of $1 \text{ kcal mol}^{-1}\cdot\text{\AA}^{-2}$, and finally (4) 50 ps NVT simulation without any restraints.¹⁵

Equilibrations were followed by 100 ns production simulations. The simulation time step was 2 fs and snapshots were saved every 20 ps. During dynamics the SHAKE algorithm was used to constrain all bonds involving hydrogen atoms.¹⁶ A 8 \AA cutoff radius was used for short-range non-bonded interactions. Long-range interactions were treated by the Particle Mesh Ewald method.^{17,18} The temperature was kept constant at 300K using Berendsen's weak coupling algorithm.¹⁵ Production simulations were carried out under NVT conditions.

Average dihedral energies and total potential energies were computed from 100ns cMD simulations and used as references for 500ns aMD simulations, respectively.¹⁹ The aMD simulations were carried out under the same conditions as described above starting from the equilibrated systems used for the cMD simulations. To enhance sampling, we applied the dual boost approach based on separate total and torsional boost potentials.¹⁹ The total boost parameter $E(\text{tot})$ was set to 2.0 times the total number of atoms plus the average total potential energy and $\alpha(\text{tot})$ to 0.2 times the total number of atoms. The torsional boost parameter $E(\text{dih})$ was set to $4.0 \text{ kcal mol}^{-1}$ times the total number of solute residues plus the average dihedral energy and $\alpha(\text{dih})$ to 0.2 times $4.0 \text{ kcal mol}^{-1}$ times the total number of solute residues.

Analysis of aMD trajectories was performed employing CPPTRAJ, and visual inspection of the MD snapshots was performed using PyMol.^{20,21} The mean probability of the two reacting atoms (cysteine sulfur and α -carbon of α -chloroacetamide) to be present within a distance of 5 \AA was determined by calculating distance frequencies between the reacting atoms using CPPTRAJ²⁰ considering the whole conformational ensemble, respectively.

1.6 Gel-based readout of reactions between proteins and peptides with dimethylamino acrylamide

All cysteine containing protein variants were incubated for 6 h at 37°C with the dimethylamino acrylamide modified peptide **Y-9L-f**. A 1 mM stock solution of ligand **Y-9L-f** in DMSO as well as 1 mM stock solutions of each protein in gel filtration buffer (100 mM NaCl, 50 mM HEPES pH 7.4, 2 mM TCEP) were prepared. The peptide stock was further diluted with buffer (100 mM NaCl, 50 mM HEPES pH 7.4)

to 20 μ M. All proteins were further diluted with the same buffer to 40 μ M. 18 μ L peptide and 18 μ L protein containing solution were preheated to 37°C for 5 min. Thereafter, peptide solutions were transferred to the protein solutions followed by intense mixing for 3 s and then incubated at 37°C for 6 h. After 30 s, 60 s, 90 s, 120 s, 150 s, 5 min, 10 min, 15 min, 30 min, 1 h, 2 h, 3 h and 6 h, 2.5 μ L of each reaction solution were pipetted to 0.5 μ L 5-fold SDS sample buffer (0.25 mM Tris pH 6.8, 10% SDS, 25% β -Mercaptoethanol, 50% glycerol, 1% 4-Bromophenol) and heated for 5 minutes at 95°C to quench the reaction. Readout was performed via SDS-PAGE according to Schagger and Jagow on 17% gels¹ and read-out of fluorescein fluorescence on a Typhoon Trio+ scanner (GE Healthcare, Freiburg, Germany) using excitation at 488 nm and detecting emission above 536 nm. Gel sections are shown in Figure S13.

1.7 HPLC-based readout of reactions between proteins and peptides with α -chloroacetamide

For the determination of initial reaction rates, the three most reactive P/L-pairs (**P(C638)** + **CI-9/13/19L-f**, respectively) as well as controls (**P(C638)** + **CI-9iL-f**; **P(C638)** + **H-9L-f**; GSH + **CI-9L-f**) were incubated for 12 h at 37°C in independent triplicates. For each triplicate 1 mM stock solutions of each ligand in DMSO as well as 1 mM stock solutions of each protein in gel filtration buffer (100 mM NaCl, 50 mM HEPES pH 7.4, 2 mM TCEP) were prepared. Additionally 5.625 mM and 22.5 μ M GSH-solutions were prepared in buffer containing 100 mM NaCl, 50 mM HEPES pH 7.4 and 45 μ M TCEP. All peptide stocks were further diluted with buffer (100 mM NaCl, 50 mM HEPES pH 7.4) to 90 μ M. All proteins were further diluted with the same buffer to 22.5 μ M. 100 μ L peptide and 800 μ L protein/GSH containing solution were preheated to 37°C for 5 min in a 96 well plate (DeepWell™ plates 1.3 ml, Nunc™ from Thermo Fisher Scientific Inc., Waltham, Massachusetts, USA). Thereafter, peptide solutions were transferred to the protein or GSH solutions followed by intense mixing for 3 s and then incubated at 37°C for 12 h. After 30 s, 60 s, 90 s, 120 s, 150 s, 5 min, 10 min, 15 min, 30 min, 1 h, 2 h, 3 h, 6 h, 9 h and 12 h, 53 μ L of each reaction solution were pipetted to 1.06 μ L TFA (final concentration 2%) to quench the reaction. Readout was performed via reversed-phase HPLC separation (Hitachi HPLC LaChrom Elite Serie system from Hitachi, Tokyo, Japan equipped with a Zorbax Eclipse, XDB-C18 reverse-phase column 4.6 · 150 mm, particle size 5 μ m from Agilent Technologies, Santa Clara, California, USA ; solvent A: H₂O with 0.1% TFA, solvent B: ACN with 0.1% TFA, gradient: 30-95% B in 10 min) coupled with UV/Vis-detection at 210 nm and 440 nm. An exemplary chromatogram is shown in Figure S11, obtained yields are listed in Table S10 and graphs for the calculation of the initial reaction rates are shown in Figure S12. For data processing see section 1.8.

1.8 Processing of HPLC measurements

For detection of reaction yields, reversed-phase HPLC separation of the reaction mixture (Hitachi HPLC LaChrom Elite Serie system from Hitachi, Tokyo, Japan equipped with a Zorbax Eclipse, XDB-C18 reverse-

phase column 4.6 x 150 mm, particle size 5 µm from Agilent Technologies, Santa Clara, California, USA ; solvent A: H₂O with 0.1% TFA, solvent B: ACN with 0.1% TFA, gradient: 30-95% B in 10 min) coupled with UV/Vis-detection at 210 nm and 440 nm was performed. Thereafter, the two assigned peaks detected at 440 nm (protein/GSH conjugated to f-labeled peptides and pure f-labeled peptides, respectively) were integrated and the yield was calculated. For initial reactivity tests, single measurements were performed. Obtained values are given in Table S7. Based on these values the heat map of initial reactivity tests was obtained as follows: For reactions without detectable conversion the detection limit was set to 2% (8 pmol). For reactions with detectable conversion, initial rates were determined. If measurements were above 30% yield (and therefore outside the linear phase) only apparent initial reaction rates could be determined. For P/L pairs with quantitative yield after less than an 1 h, an initial reaction rate of > 2 nM·s⁻¹ was assigned. The initial reaction rates are given in Table S8.

For precise kinetic measurements, the yields of three independent experiments were averaged and their SD was determined using GraphPad Prism 5.0 for Windows (GraphPad Software, San Diego California USA, www.graphpad.com) before processing. Raw data are given in Table S10. For further processing only conversion rates between 2% and 30% were used. Linear regression was performed and initial reaction rates v in nM·s⁻¹ were determined from the slope m of each regression line shown in Figure S14 using equation 1.

$$v = \frac{c \cdot m}{t} \quad (\text{eq 1})$$

with $t = 60$ min and $c = 10$ µM

Standard deviations (SD) of initial reactions rates were calculated using Gaussian error propagation with the standard deviation SD_m of each slope of the regression lines according to equation 2:

$$SD = \sqrt{\left[\left(\frac{10 \cdot c}{t}\right) \cdot SD_m\right]^2 + \left[\left(\frac{10 \cdot m}{t}\right) \cdot SD_c\right]^2 + \left(\left(\frac{10 \cdot m}{t^2}\right) \cdot SD_t\right)^2} \quad (\text{eq 2})$$

with $t = 60$ sec, $c = 10$ µM, $SD_c = 0.2$ µM, $SD_t = 2$ sec

1.9 HPLC-ESI-MS measurement of P(C638)-9L-f

For ESI-MS analysis of the reaction product from **P(C638)** with **CI-9L-f** the reaction mixture was incubated for 1 h at 37°C to ensure complete conversion. A 1 mM stock solution of **CI-9L-f** in DMSO as well as a 1 mM stock solution of **P(C638)** in gel filtration buffer (100 mM NaCl, 50 mM HEPES pH 7.4, 2 mM TCEP) were prepared. Both stocks were further diluted with buffer (100 mM NaCl, 50 mM HEPES pH 7.4) to 40 µM. 60 µL of each solution were combined, followed by fast mixing for 3 s and incubated at 37°C for 1 h. Thereafter, the reaction was quenched with 1.2 µL TFA (final concentration 1%).

Readout was performed via reversed-phase HPLC separation of the reaction mixture (1200 system equipped with a Zorbax Eclipse, XDB-C18 reverse-phase column 4.6 · 150 mm, particle size 5 µm from Agilent Technologies, Santa Clara, California, USA ; solvent A: H₂O with 0.1% TFA, solvent B: ACN with 0.1% TFA, gradient: 30-95% B in 10 min) coupled with UV/Vis-detection at 210 nm and 440 nm as well as ESI-MS (LCQ Advantage Max (Finnigan™) from Thermo Fisher Scientific Inc., Waltham, Massachusetts, USA). The chromatogram and the obtained mass spectra of **P(C638)** and **P(C638)-9L-f** are shown in Figure S15.

1.10 In gel digest and MS/MS measurement of **P(C638)-9L-f**

For in gel digest and MS/MS analysis of the reaction product from **P(C638)** with **CI-9L-f** the reaction mixture was incubated for 1 h at 37°C to ensure complete conversion. A 1 mM stock solution of **CI-9L-f** in DMSO as well as a 1 mM stock solution of **P(C638)** in gel filtration buffer (100 mM NaCl, 50 mM HEPES pH 7.4, 2 mM TCEP) were prepared. The peptide stock was further diluted with buffer (100 mM NaCl, 50 mM HEPES pH 7.4) to 200 µM. The protein was further diluted with the same buffer to 100 µM. 5 µL of each solution were combined, followed by intense mixing for 3 s and incubated at 37°C for 1 h. As control 5 µL of **P(C638)** solution were combined with 5 µL buffer including 20% DMSO. Thereafter, solutions were quenched with 1 µL TFA (final concentration 10%) and mixed with 2 µL 6x SDS sample buffer prior to heating at 95°C for 5 min. All samples were subjected to SDS-PAGE on a 17% Tris-Tricin gel according to Schagger and Jagow.¹ As control a BSA sample (5 pmol) and a protein-free gel piece were subjected to the following treatment. After sufficient separation, the gel (Figure S16a) was stained and desired protein bands were cut out with a scalpel. The gel pieces were destained by repeating the following procedure two times: 200 µl washing solution 1 (25 mM NH₄HCO₃/ACN 3:1) were added and the samples were incubated for 30 min at 37°C. The solution was removed completely and 200 µl washing solution 2 (25 mM NH₄HCO₃/ACN 1:1) were added and the samples were incubated for 15 min at 37°C. Afterwards the samples were reduced (100 µl 50 mM DTT in 25 mM NH₄HCO₃ for 45 min at 37°C) and alkylated (100 µl 55 mM iodoacetamide in 25 mM NH₄HCO₃ for 1 h at 22°C). For drying the samples two washing steps with washing solution 2 (100 µl for 15 min at 37°C) were performed and 10 µl ACN were added for 10 min at 37°C. After complete evaporation of the solvent, 15 µl digest solution (10 µl 0.1 mg/ml Trypsin solution dissolved in 10 mM HCl with 90 µl 25 mM NH₄HCO₃) were added and incubated for 15 min at 22°C. Thereafter, the gel was incubated at 30°C over night. For peptide extraction, 3.5 µl 10% TFA were added and the gel pieces were incubate for 30 min in a sonication bath at 0°C before the supernatant was removed. For further elution 20 µl ACN were added to the gel pieces for 10 min at 22°C and afterwards added to the supernatant. This solution was dried in a speedvac system and analyzed via HPLC-MS/MS. For sequence coverage see Figure S16b, for analysis of the 9L-f labeled protein fragment of **P(C638)** see Figure S16c.

For protein identification, tryptic peptides were separated and analyzed by nano-HPLC-MS/MS using an UltiMate™ 3000 RSLCnano system and a Q Exactive™ Hybrid Quadrupole-Orbitrap Mass Spectrometer equipped with a nano-spray flex ion source (Thermo Scientific, Germany) as described earlier.²² All solvents were of LC-MS grade. The lyophilized tryptic peptides were dissolved in 20 µl 0.1 % TFA in water. 3 µl of sample were injected onto a pre-column cartridge (5 µm, 100 Å, 300 µm ID x 5 mm; Dionex, Germany) using 0.1 % TFA in water as eluent with a flow rate of 30 µl/min. Desalting was performed for 5 min with eluent flow to waste followed by back-flushing of the sample during the whole analysis from the pre-column to a PepMap100 RSLC C18 nano-HPLC column (2 µm, 100 Å, 75 µm ID x 25 cm; nanoViper, Dionex) using a linear gradient starting with 95 % solvent A (0.1 % formic acid in water) vs 5 % solvent B (0.1 % formic acid in acetonitrile) and increasing to 30 % solvent B after 95 min; the flow rate was 300 nl/min.

The nano-HPLC was online coupled to the Quadrupole-Orbitrap Mass Spectrometer using a standard coated SilicaTip (ID 20 µm, Tip-ID 10 µm; New Objective, Woburn, MA, USA). Mass range of m/z 300 to 1650 was acquired with a resolution of 70,000 for full scan, followed by up to ten high energy collision dissociation (HCD) MS/MS scans of the most intense at least double charged ions.

Data evaluation was performed using the MaxQuant software (v.1.5.2.8)²³ including the Andromeda search algorithm and searching the human and *E. coli* reference proteome of the uniprot database in parallel with a small Fasta file containing just the sequences of the **P(wt)** and the **P(C638)** protein and a database containing typical contaminants.²³ The search was performed for full enzymatic trypsin cleavages allowing two miscleavages. For protein modifications, oxidation of methionine, carbamidomethylation of cysteins, cysteine modified with **CI-9L-f** (mass difference compared to unmodified cysteine: 2658.2716 g·mol⁻¹, formal addition of C₁₂₈H₁₇₉N₂₅O₃₅S to cysteine) and cysteine modified with **CI-9L-f** and cleaved C-terminal of the lysine of the modification (mass difference compared to unmodified cysteine: 1556.8702 g·mol⁻¹, formal addition of C₇₄H₁₂₉N₁₄O₂₂ to cysteine) were chosen as variable modifications. The mass accuracy for full mass spectra was set to 5 ppm and for MS/MS spectra to 20 ppm. The false discovery rates for peptide and protein identification were set to 1 %. Mass traces of the modified peptide were drawn directly from the raw-files and MS/MS spectra of the modified peptide were annotated manually.

1.11 Covalent pulldowns

1.11.1 Covalent pulldown of purified P(wt) and P(C638)

For each sample 100 µL Dynabeads M-280 (Thermo Fisher Scientific Inc., Waltham, Massachusetts, USA) were used. Bead equilibration was performed according to the manual with pulldown buffer (500 mM

NaCl, 50 mM HEPES pH 7.4, 0.01% Tween-20). After the last washing step, beads were resuspended in 50 μ L of pulldown buffer.

For incubation with peptides, 1 nmol of biotinylated peptide was added to a bead sample and incubated for 30 min at 12°C. Therefore, 1 μ L of a 1 mM peptide stock in DMSO were diluted with 49 μ L pulldown buffer. Thereafter, beads were washed three times with 500 μ L of pulldown buffer and resuspended in 50 μ L.

For protein pulldown, 50 μ L of a 20 μ M solution of both proteins was prepared in pulldown buffer and added to the resuspended beads followed by 30 min incubation at 12°C. Thereafter, the beads were washed three times with 500 μ L of pulldown buffer and resuspended in 8 μ L elution solution (50 mM Biotin in ddH₂O – note that it is important to work completely salt free). The suspension was heated to 95°C for 5 min and shortly spinned down before the supernatant was removed and mixed with 2 μ L 5x SDS loading buffer (0.25 mM Tris-HCl pH 6.8, 10% (w/v) SDS, 25% β -Mercaptoethanol, 50% Glycerin, 1% (w/v) Bromophenol Blue).

As input controls, solutions containing either only the proteins or the proteins combined with ligand **CI-9L-bt** were prepared. 1 nmol of protein was incubated with afore mentioned bead samples. As input control 0.2 nmol protein was used (this equals the maximum capacity of used bead aliquots) either with or without 800 pmol of ligand **CI-9L-bt** were mixed with pulldown buffer 1 to obtain a final volume of 8 μ L and incubated at 37°C for 1 h to ensure complete reaction of **P(C638)** with **CI-9L-bt**. Thereafter, samples were mixed with 2 μ L of 5x SDS loading buffer. For gel analysis of pulldown all samples were heated to 95°C for 5 min and 2 μ L of each sample were processed on a 17% Tris-Tricin gel according to Schagger and Jagow.¹ Gel electrophoresis was performed at 100 V for 90 min. The coomassie stain of the full gel is shown in Figure S17.

1.11.2 Covalent pulldown of **P(wt)**-Cherry and **P(C638)**-Cherry from Hek293 lysates

To obtain lysates for this pulldown experiments two pmCherry N1 vectors containing either **P(wt)** or **P(C638)** as C-terminal fusion partners of Cherry were prepared via a standard restriction ligation protocol (see Table S1 for primer sequences and properties, Table S3 for protein sequences and Table S5 for protein parameters). Obtained vectors were sequenced at StarSEQ[®] GmbH (Mainz, Germany) to ensure correctness. For pulldown experiments, Hek293 cells were stable transfected with constructs encoding **P(wt)**-Cherry or **P(C638)**-Cherry, respectively. This was performed with Lipofectamin 3000 reagent (Thermo Fisher Scientific Inc., Waltham, Massachusetts, USA) on confluent grown cells. Briefly 200 ng plasmid DNA in ddH₂O were premixed with 55 μ L Opti-MEM[®] (Thermo Fisher Scientific Inc., Waltham, Massachusetts, USA) and 2.2 μ L 3000 reagent before adding 2.2 μ L Lipofectamin reagent premixed with 55 μ L Opti-MEM. After 5 min incubation at room temperature,

50 μ L of this mixture were added to one well of a 24-well-plate (standard growth surface for adherent cells, pyrogen-free, non-cytotoxic from Sarstedt AG & Co., Nümbrecht, Germany) in which cells were grown to approximately 80% confluence. Cells were incubated for approximately 60 h at 37°C and 5% CO₂ in a Steri-Cylce CO₂ incubator (Thermo electron corporation, Langenselbond, Germany) before G418 was added to a concentration of 200 ng· μ L⁻¹. Single colonies were picked and grown until confluency was reached in 60x15 mm dishes (standard growth surface for adherent cells, pyrogen-free, non-cytotoxic from Sarstedt AG & Co., Nümbrecht, Germany). For lysis, these dishes were harvested after trypsin treatment and resuspended in lysis buffer (15 mM NaCl, 5 mM Tris, 100 μ M EDTA, 0.1% NP-40, 0.05% Na-deoxycholic acid, 0.01% Sodium dodecyl sulfate) before they were subjected to ultrasonification (2 · 10 sec at 10% and 4°C).

For each pulldown sample, 400 μ L beads were used and bead equilibration was performed according to the manual with pulldown buffer (500 mM NaCl, 50 mM HEPES pH 7.4, 0.01% Tween-20). After the last washing step the beads were resuspended in 400 μ L of pulldown buffer. For incubation with peptides, 4 nmol of each peptide were added to a bead sample and incubated for 30 min at 12°C. Therefore, 4 μ L of a 1 mM peptide stock in DMSO were diluted with 396 μ L pulldown buffer. Thereafter, the beads were washed three times with 500 μ L of pulldown buffer and resuspended in 200 μ L. For pulling of proteins, the lysates were diluted to 2 mg/mL total protein concentration with pulldown buffer in 200 μ L and added to the resuspended beads followed by 3 h incubation at 12°C. Thereafter, the beads were washed three times according to the manual with 500 μ L of pulldown buffer and resuspended in 20 μ L 1x SDS sample buffer.

As input controls solutions containing only lysate were prepared. As the binding capacity of Dynabeads M-280 for proteins of the size of P-Cherry is not known, we estimated that only 1% of the used input could bind to the beads. Therefore, 0.25 pmol of Cherry were mixed with water to obtain a final volume of 16 μ L for both lysates. Afterwards, the samples were mixed with 4 μ L of 5x SDS loading buffer (0.25 mM Tris-HCl pH 6.8, 10% (w/v) SDS, 25% β -Mercaptoethanol, 50% Glycerin, 1% (w/v) Bromophenol Blue).

For analysis of the pulldown, all samples were heated to 95°C for 5 min and 10 μ L were processed on a 12% Tris-Tricin gel according to Schägger and Jagow.¹ Gel electrophoresis was performed at 100 V for 120 min. Thereafter, the gel was blotted onto nitrocellulose membrane (Amersham Protran 0.45 NC 300mmx4m from GE Healthcare Europe GmbH, Freiburg, Germany) in semi-dry fashion using transfer buffer (10% MeOH, 20 mM Tris pH 8.3, 100 mM Glycin) for 40 min with 200 mA. The membrane was blocked for 1 h at room temperature with 5% milk powder in TBS-T (20 mM Tris, 150 mM NaCl, 1% Tween-20). After washing the membrane two times with TBS-T for 5 min at room temperature, the primary antibody (anti-mCherry from Novus Biologicals, Littleton, Colorado, USA; article number NBP1-

96752, dilution 1:1000, 0.02% NaN₃, 3% milk powder in 10 mL TBS-T) was incubated for 1 h at room temperature. Following three washing steps the membrane was incubated for 1 h at room temperature with the secondary alkaline phosphatase coupled antibody (from cell signaling, Danvers, Massachusetts, USA; article number 7056, dilution 1:10000, 0.02% NaN₃, 3% milk powder in 10 mL TBS-T) and again washed five times with TBS-T at room temperature. For development, the membrane was incubated with BCIP/NBT (Merck Millipore, Darmstadt, Germany) and quenched with H₂O after sufficient band intensity arised. The full membrane is shown in Figure S18.

1.12 Labeling reactions in cell lysates

To obtain *E. coli* lysates without overexpressed proteins a 15 mL culture of LB media was inoculated with an aliquot of non-transformed *E. coli* BL21 DE3 (gold) cells. After incubation over night at 37°C cells were harvested via centrifugation (3.000 rcf, 4°C, 15 min.) and lysed with ultrasonification (3 · 10 sec at 10% and 4°C) in 0.6 mL lysis buffer (500 mM NaCl, 50 mM HEPES pH 7.4, 2 mM TCEP).

To obtain purified proteins **P(C638)**-Cherry and **P(wt)**-Cherry DNS sequences for proteins P(C638) and P(wt) were cloned into a GFP-containing pGEX-4T5 vector. After exchange of GFP to Cherry via *in vivo* cloning²⁴ both proteins were expressed in *E. coli* BL21 DE3 (gold) cells and purified analog to non-fused protein variants (see section 1.1 of SI methods). Some contaminations including shortened versions of **P**-cherrys could not be removed by this purification strategy. Therefore, concentration of **P**-cherry fusion constructs was determined via cherry absorption at 587 nm ($\epsilon = 72.000 \text{ L} \cdot \text{mol}^{-1} \cdot \text{cm}^{-1}$).²⁵

For labeling reactions in cell lysates, a 1 mM stock solution of ligand **CI-9L-f** in DMSO as well as 1 mM stock solutions of each protein in gel filtration buffer (100 mM NaCl, 50 mM HEPES pH 7.4, 2 mM TCEP) were prepared. The peptide stock was further diluted with buffer (100 mM NaCl, 50 mM HEPES pH 7.4) to 80 μM . Both proteins were spiked into *E. coli* lysate and further diluted with the same buffer to 22.9 μM cherry fusion proteins and 10 $\text{mg} \cdot \text{mL}^{-1}$ of total protein concentration, respectively. 16.25 μL peptide and 113.75 μL protein containing solution were preheated to 37°C for 5 min. Thereafter, peptide solutions were transferred to protein solutions followed by intense mixing for 3 s and then incubated at 37°C for 10 min. After 30 s, 60 s, 90 s, 120 s, 150 s and 5 min, 2.5 μL of each reaction solution were pipetted to 0.5 μL 5-fold SDS sample buffer (0.25 mM Tris pH 6.8, 10% SDS, 25% β -Mercaptoethanole, 50% glycerol, 1% 4-Bromophenole) and heated for 5 minutes at 95°C to quench the reaction. Readout was performed via SDS-PAGE on 15% gels according to Schagger and Jagow¹ and read-out of fluorescein fluorescence on a Typhoon Trio+ scanner (GE Healthcare, Freiburg, Germany) using excitation at 488 nm and detecting emission above 536 nm Gels are shown in Figure S19.

1.13 Translocation of P(C638)-Cherry in living cells

For translocation experiments, HeLa cells were transiently transfected with constructs encoding **P(wt)**-Cherry or **P(C638)**-Cherry. This was performed in suspension using XtremeGENE (Roche Diagnostics Deutschland GmbH, Mannheim, Germany). 2 µg Plasmid-DNA in ddH₂O were premixed with 200 µL Opti-MEM® (Thermo Fisher Scientific Inc., Waltham, Massachusetts, USA) before adding 2 µL XtremeGENE reagent. After 15 min incubation at room temperature 200,000 cells were added and the cell suspension was carefully mixed before adding it to 2 mL DMEM (w: 4.5 g/L Glucose, w: L-Glutamine, w: sodium pyruvate, w: 3.7 g·L⁻¹ NaHCO₃ from PAN-Biotech GmbH, Aidenbach, Germany) supplemented with 10% FCS (Sera Plus, Special processed, Virus and mycoplasma tested from PAN-Biotech GmbH, Aidenbach, Germany) and NEAA's (MEM NEAA (100x) w/o: L-Glutamine from PAN-Biotech GmbH, Aidenbach, Germany) in a glass bottom dish (diameter 35 mm, poly-D-lysine coated, glass No. 1.0, glass diameter 14 mm from MatTek corporation, Ashburne, Massachusetts, USA). Cells were incubated for approximately 16 h at 37°C and 5% CO₂ in a Steri-Cylce CO₂ incubator (Thermo electron corporation, Langenselbond, Germany).

Translocation experiments were performed with a LSM 510 Meta confocal microscope (Zeiss, Oberkochen, Germany) equipped with a CO₂ incubator, a heating unit, a humidifier and a microinjection system (a FemtoJet unit for pressure supply combined with an InjectMan NI2 unit, both from Eppendorf, Hamburg, Germany). For all experiments 37°C, 5% CO₂ and 95% humidity equally to the cell incubator were chosen to reduce cellular stress.

10 mM stock solutions of peptides **f-MA**, **CI-9L-MA** and **CI-9iL-MA** for microinjection were prepared in DMSO under steril conditions. For injection of **f-MA** a 1:10-fold dilution was prepared with DMSO and centrifuged for 15 min at 16 rcf. Only the supernatant was used for injection. For injection of peptides, stock solutions were diluted 1:10-fold and fluorescein was added to a final concentration of 1 mg/mL as coinjector. The compensation pressure was set to 20 hPa, while the injection pressure was varied between 100 hPa and 300 hPa. Injection time was set to 0.5 s.

Cell pictures were taken approximately 10 min before and 60 min after injection with changing laser settings to find the best signal-to-noise-ratio for each cell. Therefore, the total fluorescence intensity varies between different cells and cannot be used for absolute quantification. Pictures were further processed with ImageJ to obtain plots of the Cherry intensities throughout the cells. For this purpose, a line with a width of 50 pixels was drawn traversing the whole cell. The intensity profile corresponding to this line was plotted with ImageJ for each cell before and 1 h after the injection of the peptide and normalized with regard to the intensity in the middle of each cell. For pictures see Figure 4, Figure S20-23.

4 REFERENCES

- (1) Schagger, H., and von Jagow, G. (1987) Tricine-sodium dodecyl sulfate-polyacrylamide gel electrophoresis for the separation of proteins in the range from 1 to 100 kDa. *Anal. Biochem.* 166, 368–379.
- (2) Gasteiger, E., Hoogland, C., Gattiker, A., Duvaud, S., Wilkins, M. R., Appel, R. D., and Bairoch, A. (2005) Protein Identification and Analysis Tools on the ExPASy Server, in *The Proteomics Protocols Handbook* (Walker, J. M., Ed.), pp 571–607. Humana Press, Totowa, NJ.
- (3) Bruschweiler, S., Konrat, R., and Tollinger, M. (2013) Allosteric communication in the KIX domain proceeds through dynamic repacking of the hydrophobic core. *ACS Chem. Biol.* 8, 1600–1610.
- (4) (2014) Maestro. Schrödinger, LLC, New York, NY.
- (5) Case, D. A. Berryman, J. T. Betz, R. M. Cerutti, D. S. Cheatham, T. E. III, Darden, T. A. Duke, R. E. Giese, T. J. Gohlke, H. Goetz, A.W. Homeyer, N. Izadi, S. Janowski, P. Kaus, J. Kovalenko, A. Lee, T. S. LeGrand, S. Li, P. Luchko, T. Luo, R. Madej, B., S. F. (2015) AMBER14. University of California, San Francisco.
- (6) Götz, A. W., Williamson, M. J., Xu, D., Poole, D., Le Grand, S., and Walker, R. C. (2012) Routine microsecond molecular dynamics simulations with AMBER on GPUs. 1. Generalized born. *J. Chem. Theory Comput.* 8, 1542–1555.
- (7) Salomon-Ferrer, R., Götz, A. W., Poole, D., Le Grand, S., and Walker, R. C. (2013) Routine microsecond molecular dynamics simulations with AMBER on GPUs. 2. Explicit solvent particle mesh ewald. *J. Chem. Theory Comput.* 9, 3878–3888.
- (8) Wang, J., Wolf, R. M., Caldwell, J. W., Kollman, P. A., and Case, D. A. (2004) Development and testing of a general amber force field. *J. Comput. Chem.* 25, 1157–1174.
- (9) Bayly, C. I., Cieplak, P., Cornell, W., and Kollman, P. A. (1993) A well-behaved electrostatic potential based method using charge restraints for deriving atomic charges: the RESP model. *J. Phys. Chem.* 97, 10269–10280.
- (10) Frisch, M. J., Trucks, G. W., Schlegel, H. B., Scuseria, G. E., Robb, M. A., Cheeseman, J. R., Scalmani, G., Barone, V., Mennucci, B., Petersson, G. A., Nakatsuji, H., Caricato, M., Li, X., Hratchian, H. P., Izmaylov, A. F., Bloino, J., Zhen, G., Sonnenberg, J. L., Hada, M., Ehara, M., Toyota, K., Fukuda, R., Hasegawa, J., Ishida, M., Nakajima, T., Honda, Y., Kitao, O., Nakai, H., Vreven, T., Montgomery, J. A. J., Peralta, J. E., Ogliaro, F., Bearpark, M., Heyd, J. J., Brothers, E., Kudin, K. N., Staroverov, V. N., Kobayashi, R., Normand, J., Raghavachari, K., Rendell, A., Burant, J. C., Iyengar, S. S., Tomasi, J., Cossi, M., Rega, N., Millam, J. M., Klene, M., Know, J. E., Cross, J. B., Bakken, V., Adamo, C., Jaramillo, J., Gomperts, R., Stratmann, R. E., Yazyev, O., Austin, A. J., Cammi, R., Pomelli, C., Ochterski, J. W., Martin, R. L., Morokuma, K., Zakrzewski, V. G., Voth, G. A., Salvador, P., Dannenberg, J. J., Dapprich, S., Daniels, A. D., Farkas, Ö., Foresman, J. B., Ortiz, J. V., Cioslowski, J., and Fox, D. J. (2009) Gaussian 09. Gaussian Inc., Wallingford, CT.
- (11) Wang, J., Wang, W., Kollman, P. A., and Case, D. A. (2006) Automatic atom type and bond type perception in molecular mechanical calculations. *J. Mol. Graph. Model.* 25, 247–260.
- (12) Hornak, V., Abel, R., Okur, A., Strockbine, B., Roitberg, A., and Simmerling, C. (2006) Comparison of multiple Amber force fields and development of improved protein backbone parameters. *Proteins* 65, 712–725.
- (13) Maier, J. A., Martinez, C., Kasavajhala, K., Wickstrom, L., Hauser, K. E., and Simmerling, C. (2015) ff14SB: Improving the accuracy of protein side chain and backbone parameters from ff99SB. *J. Chem. Theory Comput.* 11, 3696–3713.
- (14) Jorgensen, W. L., Chandrasekhar, J., Madura, J. D., Impey, R. W., and Klein, M. L. (1983) Comparison of simple potential functions for simulating liquid water. *J. Chem. Phys.* 79, 926–935.
- (15) Berendsen, H. J. C., Postma, J. P. M., van Gunsteren, W. F., DiNola, A., and Haak, J. R. (1984) Molecular dynamics with coupling to an external bath. *J. Chem. Phys.* 81, 3684–3690.

- (16) Ryckaert, J.-P., Ciccotti, G., and Berendsen, H. J. C. (1977) Numerical integration of the cartesian equations of motion of a system with constraints: molecular dynamics of n-alkanes. *J. Comput. Phys.* **23**, 327–341.
- (17) Darden, T., York, D., and Pedersen, L. (1993) Particle mesh Ewald: An N·log(N) method for Ewald sums in large systems. *J. Chem. Phys.* **98**, 10089–10092.
- (18) Essmann, U., Perera, L., Berkowitz, M. L., Darden, T., Lee, H., and Pedersen, L. G. (1995) A smooth particle mesh Ewald method. *J. Chem. Phys.* **103**, 8577–8593.
- (19) Pierce, L. C. T., Salomon-Ferrer, R., Augusto F. de Oliveira, C., McCammon, J. A., and Walker, R. C. (2012) Routine access to millisecond time scale events with accelerated molecular dynamics. *J. Chem. Theory Comput.* **8**, 2997–3002.
- (20) Roe, D. R., and Cheatham, T. E. (2013) PTRAJ and CPPTRAJ: Software for Processing and Analysis of Molecular Dynamics Trajectory Data. *J. Chem. Theory Comput.* **9**, 3084–3095.
- (21) The PyMOL Molecular Graphics System. Schrödinger, LLC.
- (22) Vendrell-Navarro, G., Rúa, F., Bujons, J., Brockmeyer, A., Janning, P., Ziegler, S., Messegue, A., and Waldmann, H. (2015) Positional Scanning Synthesis of a Peptoid Library Yields New Inducers of Apoptosis that Target Karyopherins and Tubulin. *ChemBioChem* **16**, 1580–1587.
- (23) Cox, J., and Mann, M. (2008) MaxQuant enables high peptide identification rates, individualized p.p.b.-range mass accuracies and proteome-wide protein quantification. *Nat. Biotechnol.* **26**, 1367–1372.
- (24) Oliner, J. D., Kinzler, K. W., and Vogelstein, B. (1993) In vivo cloning of PCR products in *E. coli*. *Nucleic Acids Res.* **21**, 5192–5197.
- (25) Olenych, S. G., Claxton, N. S., Ottenberg, G. K., and Davidson, M. W. (2007) The fluorescent protein color palette. *Curr. Protoc. Cell Biol. Chapter 21*, Unit 21.5.